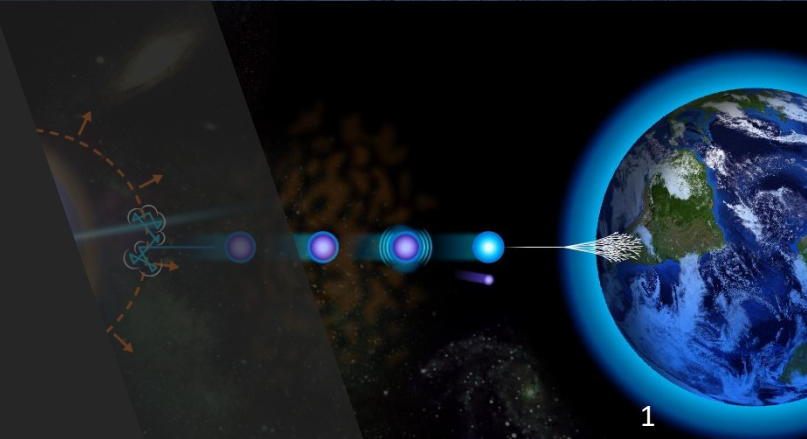


Eiji Kido

Riken, ABBL

Observation of Ultra-High-Energy Cosmic Rays and photo-nuclear reactions for the interpretation



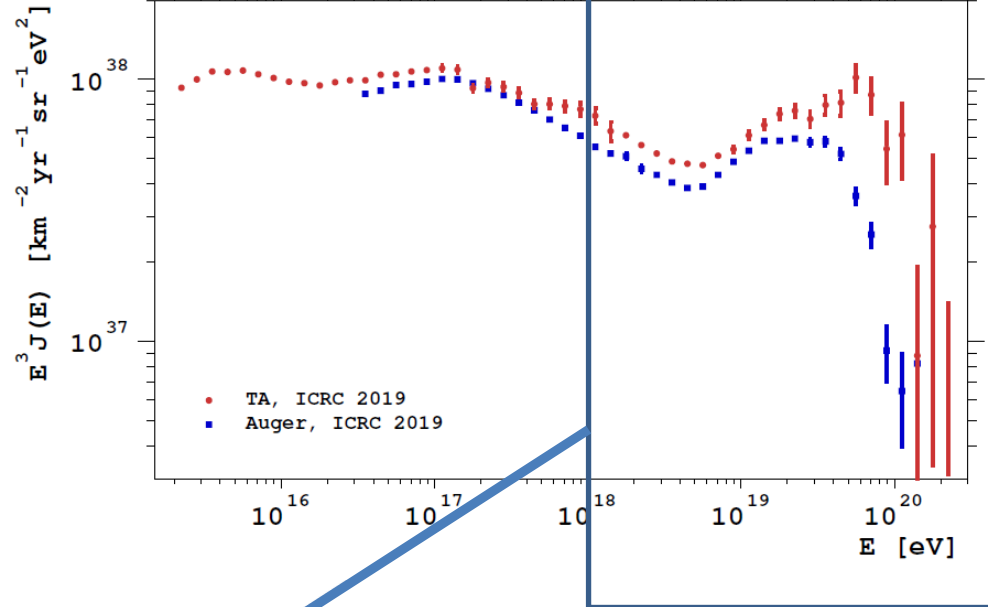
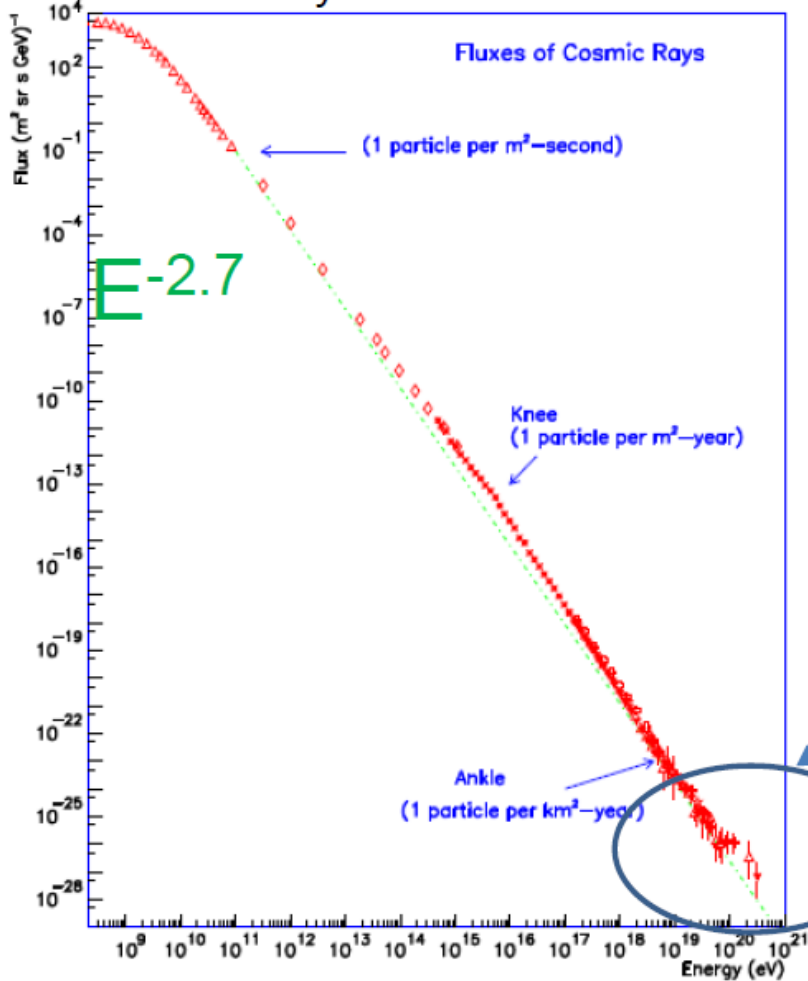
Outline

- Ultra-High-Energy Cosmic Rays (UHECRs)
- Observation of UHECRs
 - Telescope Array (TA)
 - Pierre Auger (Auger)
- Recent Results
 - Energy Spectrum
 - Composition
 - Anisotropy
- Ongoing Upgrades
 - TAx4
 - AugerPrime
- Interpretation of the Experimental Data
 - Review of the Interpretation
 - PANDORA Project
 - Impact of Photo-Nuclear Reactions on the Interpretation
 - Future Prospect
- Summary

Ultra-High-Energy Cosmic Rays (UHECRs)

Ultra-High-Energy Cosmic Rays

Differential energy spectrum of cosmic rays



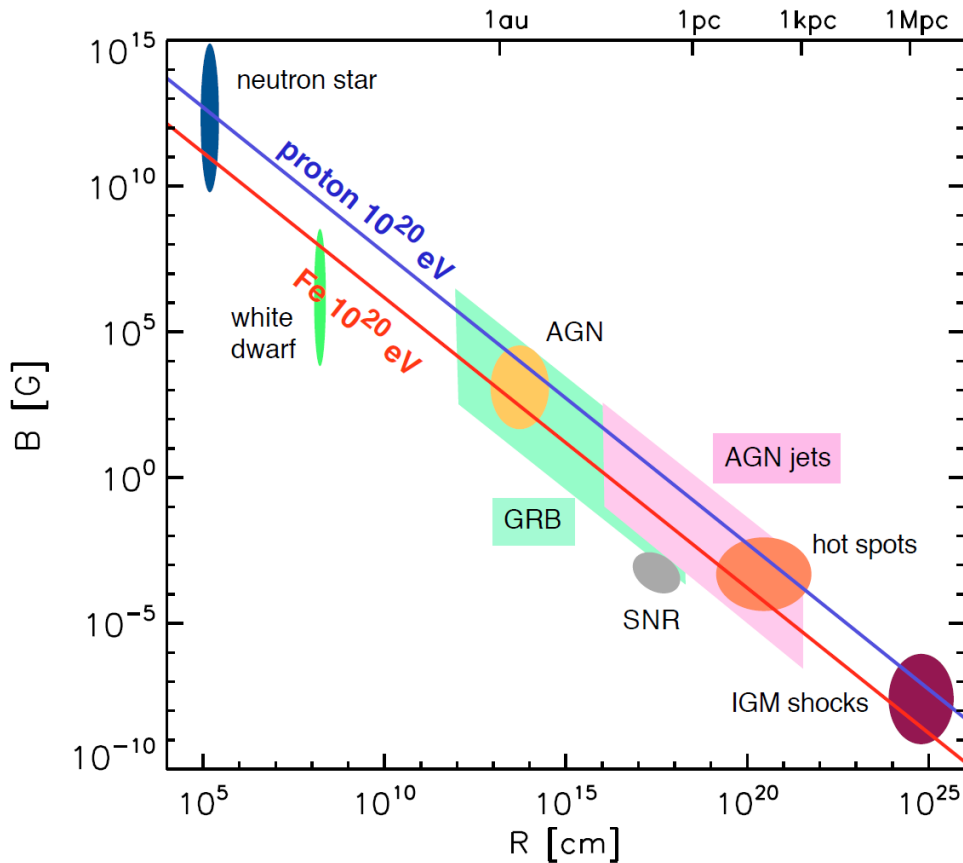
Energy > 1 EeV (1 EeV = 10^{18} eV)

Small number of events:

$\sim 10^{-3} \text{ km}^{-2} \text{ yr}^{-1}$ ($E > 10^{20}$ eV)

Cosmic ray sources are uncertain.

Hillas Diagram

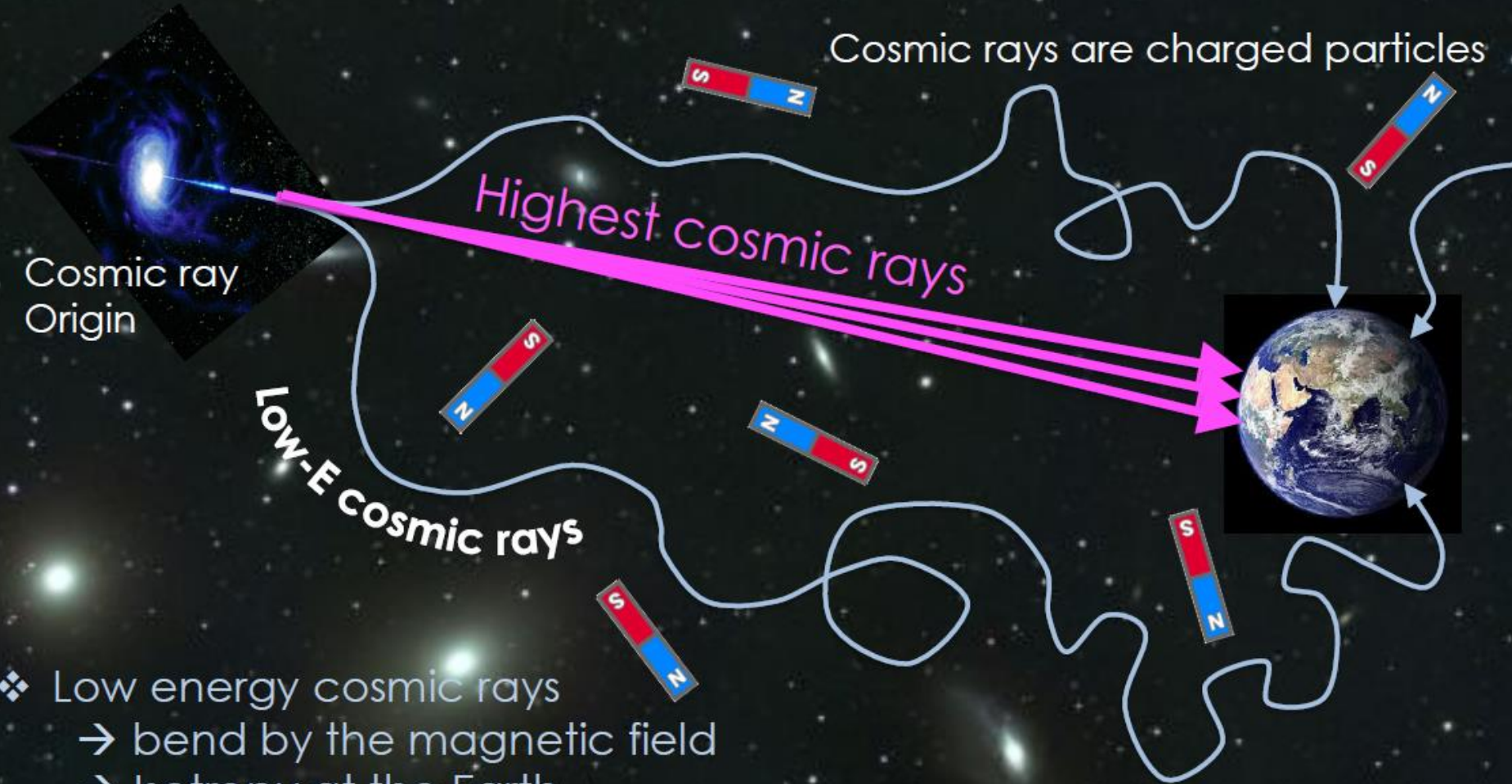


- Larmor radius

$$R_L = 100 \text{ kpc} (1/Z) (\mu\text{G}/B)(E/100 \text{ EeV})$$

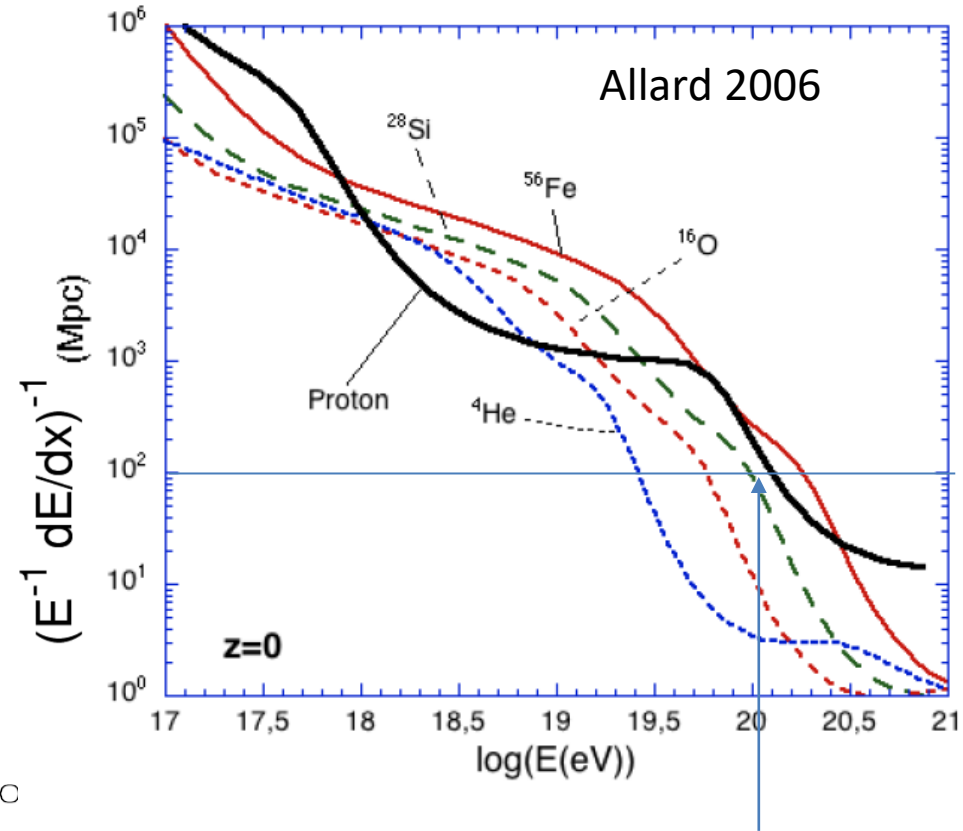
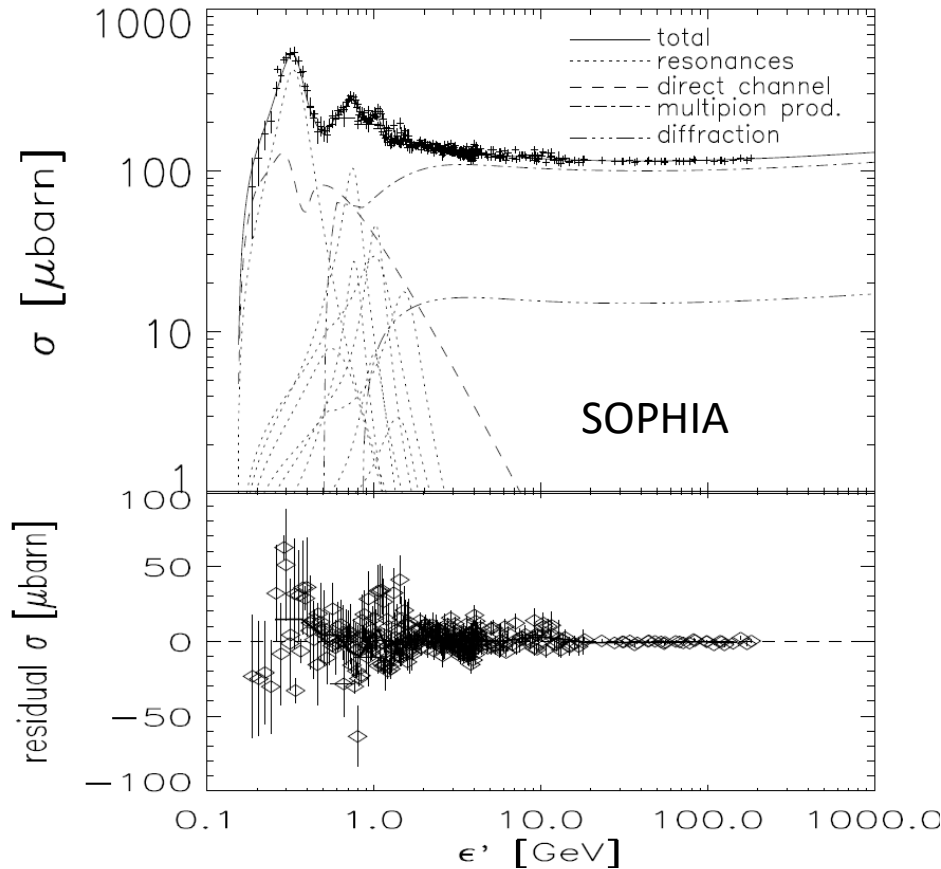
- Magnetic fields of the sources confine cosmic ray particles up to the energies
 (Blue: $E_{\text{max}} = 10^{20} \text{ eV}$, $Z=1$)
 (Red: $E_{\text{max}} = 10^{20} \text{ eV}$, $Z=26$)
 → candidates of sources

Arrival Directions



- ❖ Low energy cosmic rays
 - bend by the magnetic field
 - Isotropy at the Earth
- ❖ Highest energy cosmic rays
 - Almost go straight against magnetic field
 - Possible to find cosmic-ray origin directly

UHECR Proton Interactions



GZK cutoff (photopion production)

$\mathbf{p} + \gamma \rightarrow \mathbf{p} (\mathbf{n}) + \pi^0 (\pi^+)$ cross section

opens at $E_p > 7 \times 10^{19} \text{eV}$ with

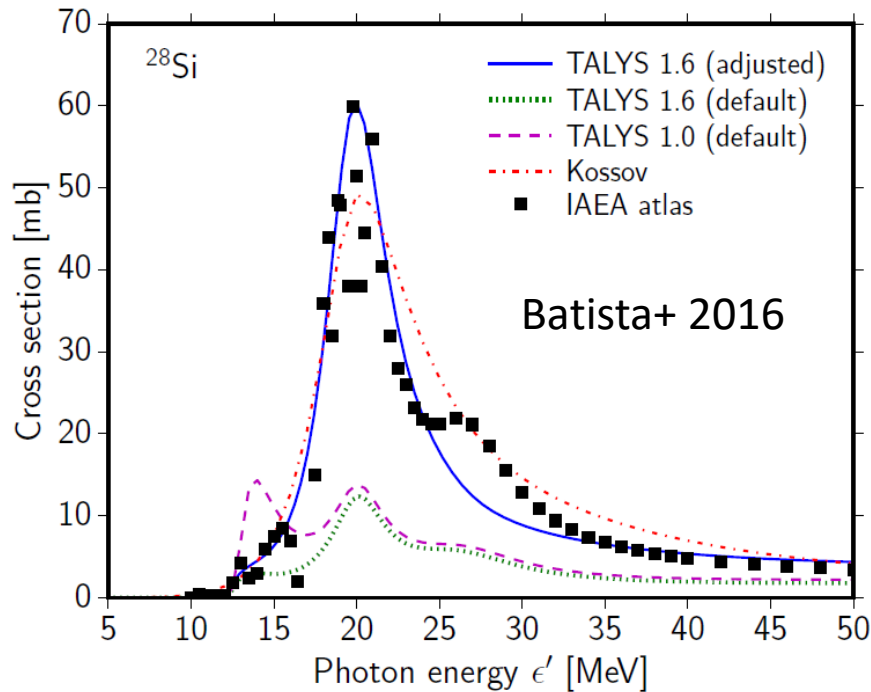
$E_{\gamma, \text{CMB}} \sim 2.4 \times 10^{-4} \text{eV}$

$(\Gamma_{\text{proton}} > 7 \times 10^9)$

Small energy loss length $< 100 \text{ Mpc}$
at the highest energies

→ Sources are limited in the local universe.

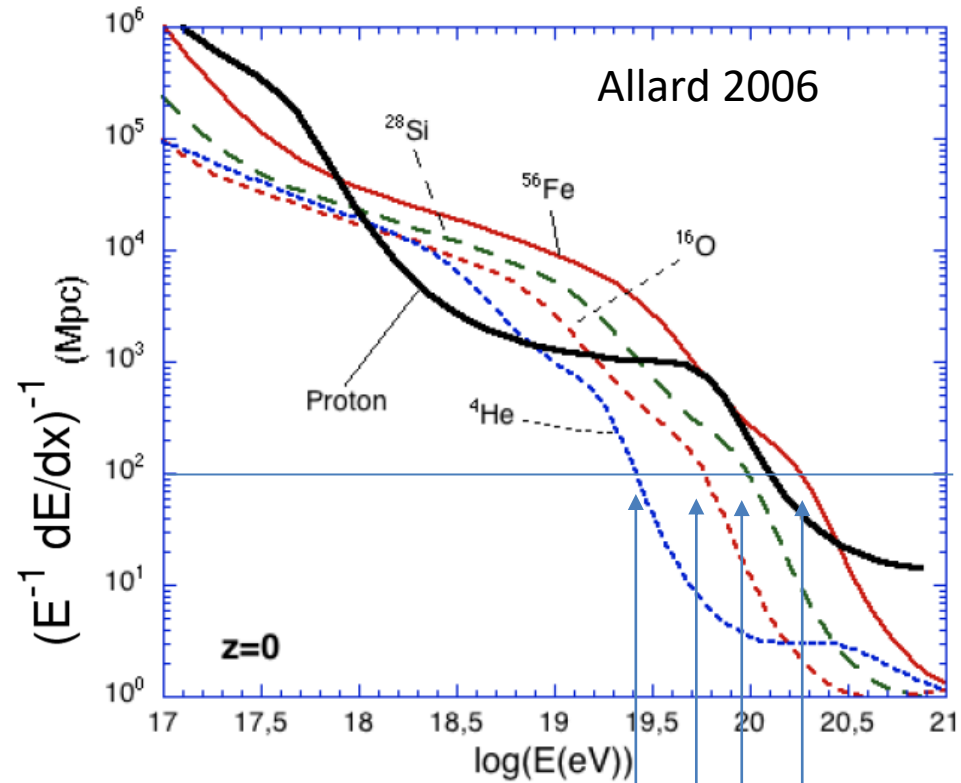
UHECR Nuclei Interactions



Photodisintegration

$A + \gamma \rightarrow (A-1) + p (n)$ cross section opens at $\Gamma_A \gtrsim 7 \times 10^8$ with CMB $E_A = A \times m_p c^2 \Gamma_A$

Typical photon energy of Giant Dipole Resonance (GDR) peak in the nucleon rest frame is $< 30-50$ MeV.



Small energy loss length < 100 Mpc at the highest energies
 \rightarrow Sources are limited in the local universe.

Motivation to observe highest energy cosmic rays

- Cosmic ray sources are uncertain
- Smaller deflection angles ($\propto 1/E$)
- Sources are limited in the local universe
(\sim a few tens of Mpcs)
 - anisotropy in arrival directions
 - origin of cosmic rays
- Difficulty: To obtain
high statistics ($\sim E_{\text{th}}^{-2}$ above E_{th})

Observation of UHECRs

UHECR Detectors

Air shower:

When cosmic ray interact with nuclei in atmosphere, many secondary particles are generated.

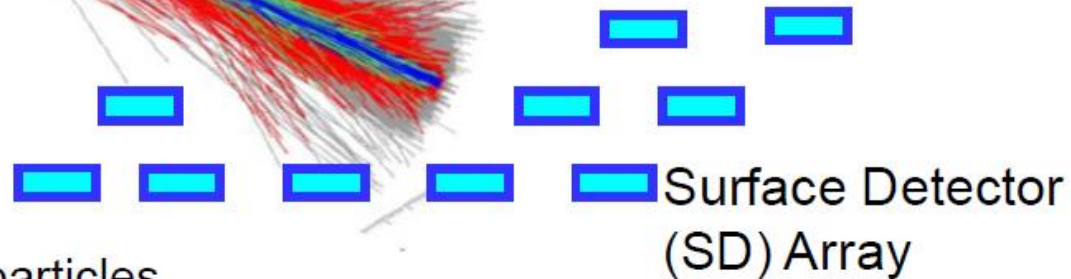
Fluorescence detectors (FDs)



Fluorescence light from the excited nitrogen by air shower particles

dN/dX

Slant depth



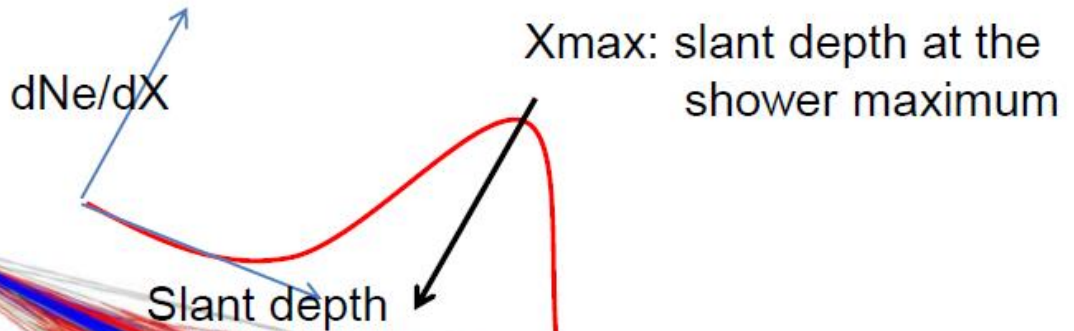
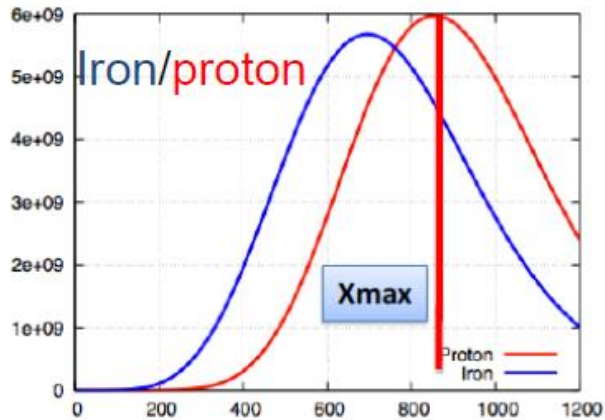
Detect air shower particles

Surface Detector (SD) and Fluorescence Detector (FD)

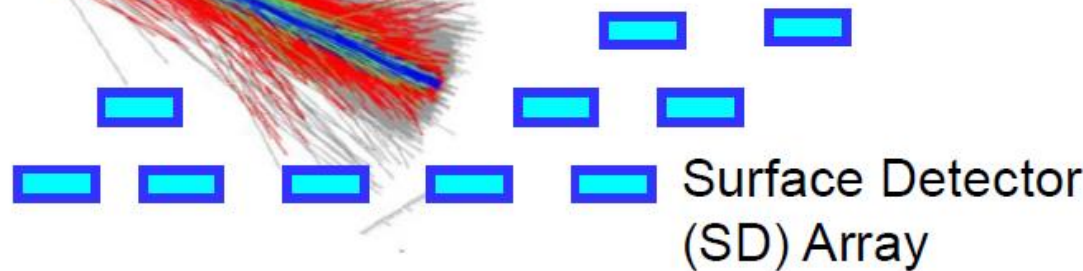
cover large area and detect the air shower.

→ Large detection area ($\sim 1000 \text{ km}^2$) is realized.

UHECR Detectors



Fluorescence detectors (FDs)



Surface Detector (SD) Array

- SD: Regardless of weather condition, high duty cycle and wide FoV → high statistics ($\sim FD \times 10$) → Anisotropy & Spectral shape
- FD: limited to clear moonless night.

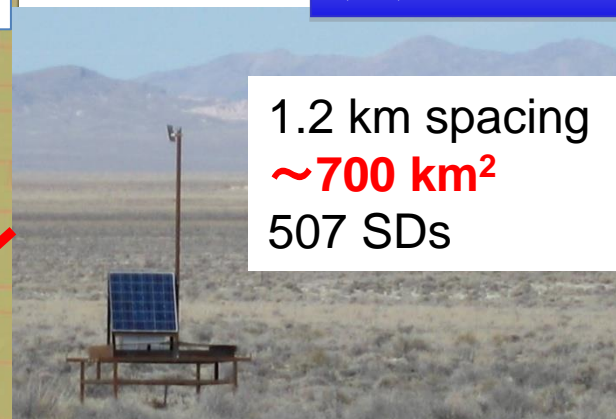
Longitudinal development of air shower → Mass composition (X_{max})

Measure the energy deposit calorimetrically → absolute energy scale

TA Detectors

Surface Detector (SD)

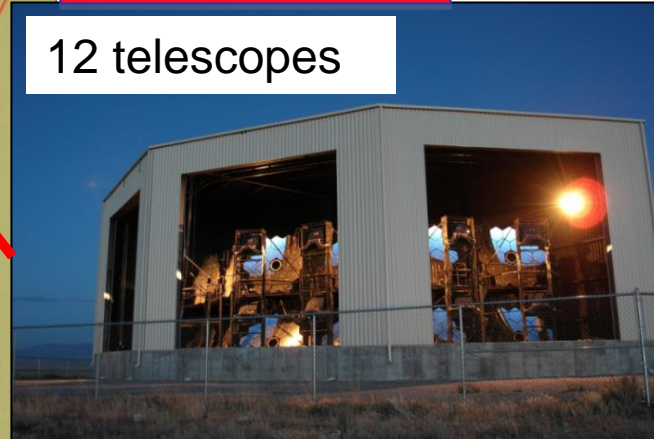
1.2 km spacing
~700 km²
507 SDs



- **Largest cosmic-ray observatory in the northern hemisphere**
- **Hybrid observation by SD and FD**

Fluorescence Detector (FD) station

12 telescopes



FD station

MDFD

TALE SD array

SD array

Latitude 39.30° N
Longitude 112.91° W
Height: 1382 m

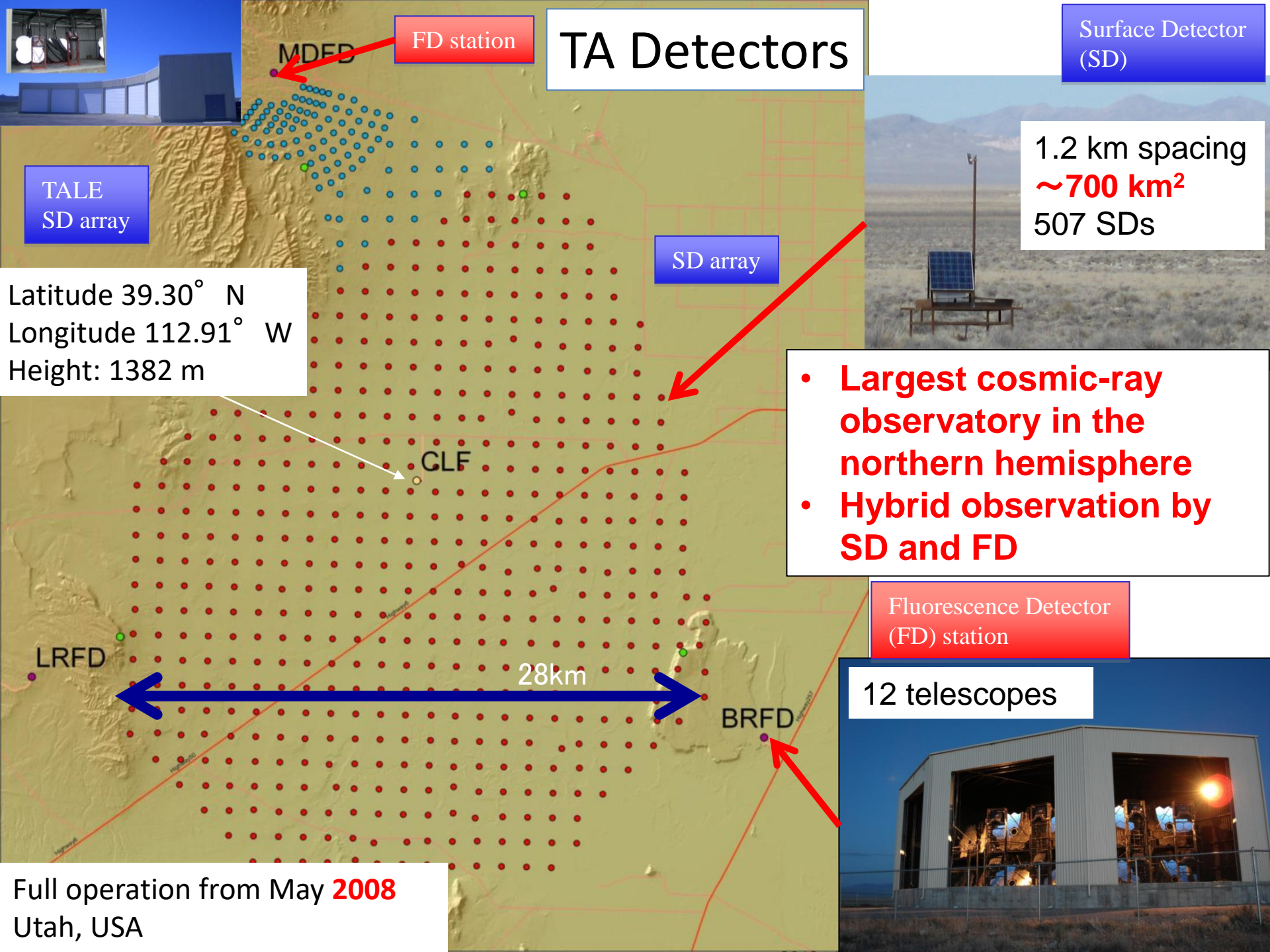
GLF

LRFD

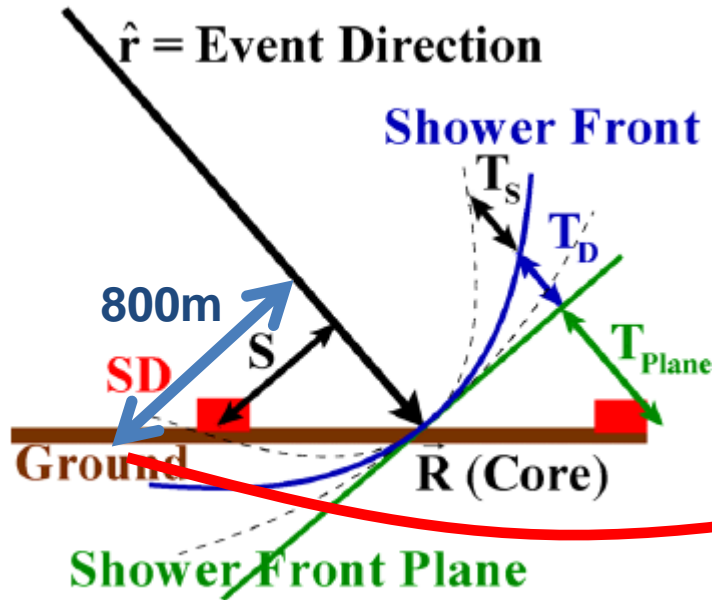
28km

BRFD

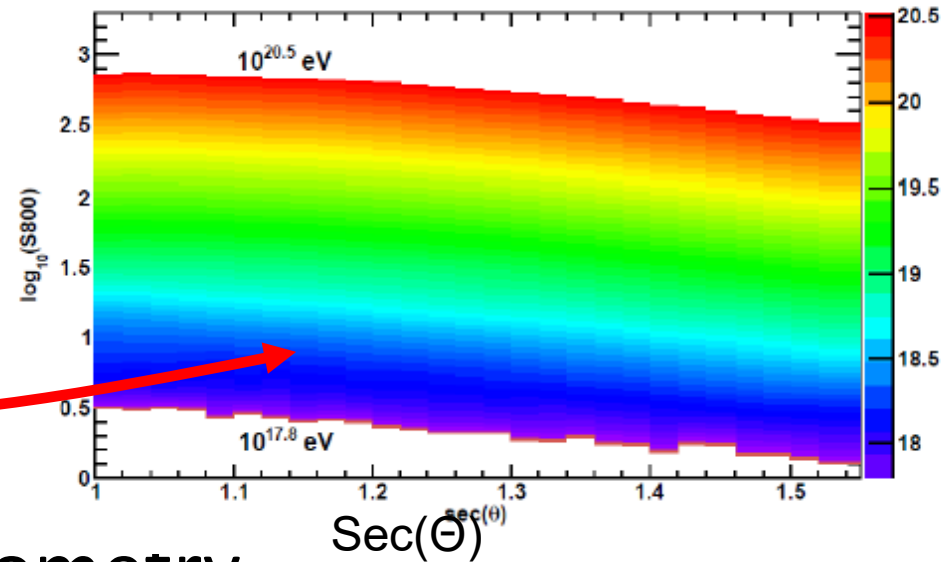
Full operation from May **2008**
Utah, USA



Event Reconstructions with SDs



$\text{Log}_{10}(S(800))$



- Timing fit \rightarrow Shower Geometry
- Lateral distribution fit $\rightarrow S(800) \rightarrow$ Energy from MC
 \rightarrow rescale to calorimetrically measured E_{FD} using

SD and FD hybrid events

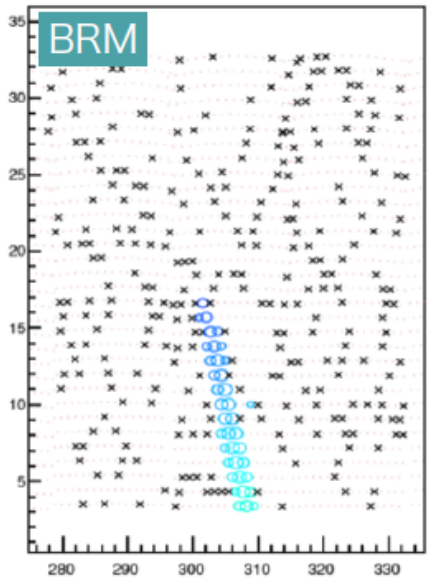
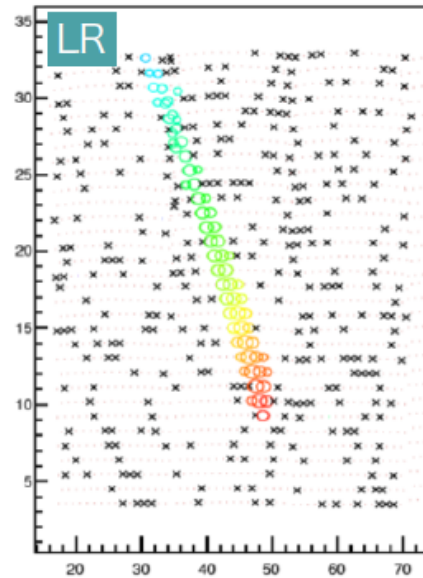
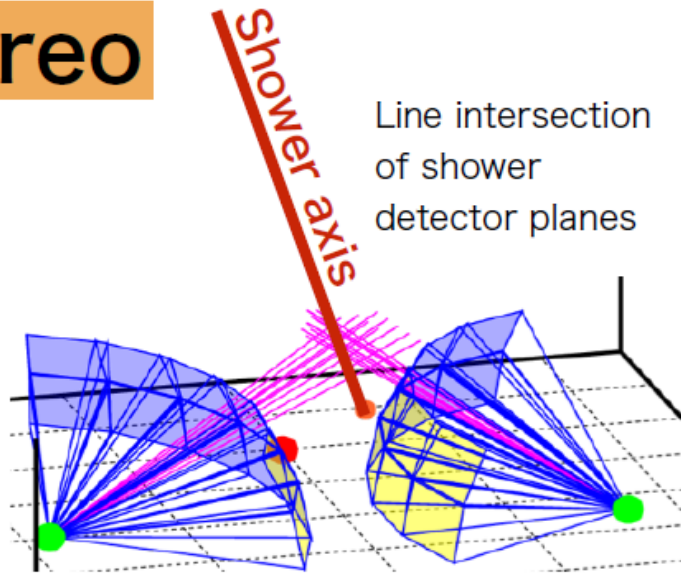
$S(800)$: energy depositions which are converted in VEM unit.

Event reconstruction

S. Ogio,
ICRC2019

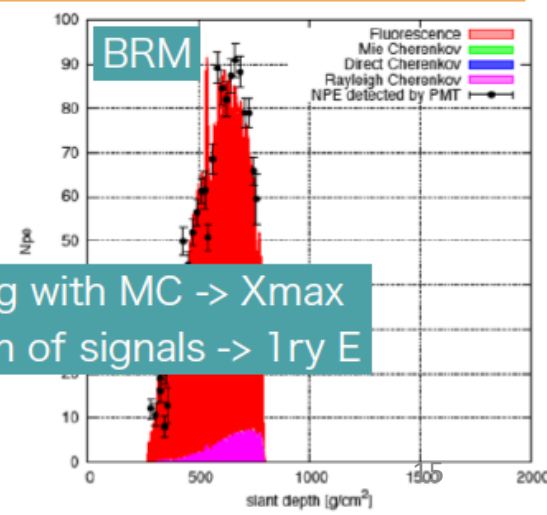
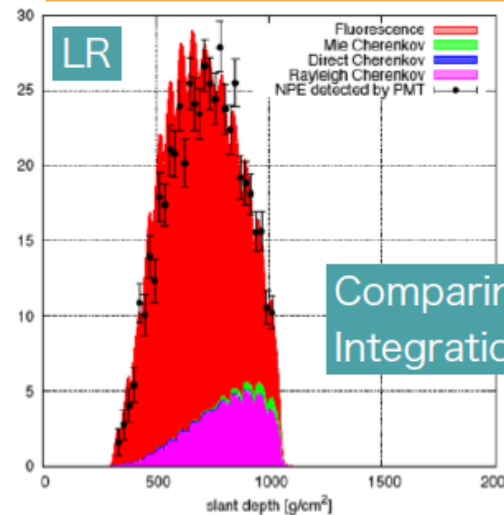
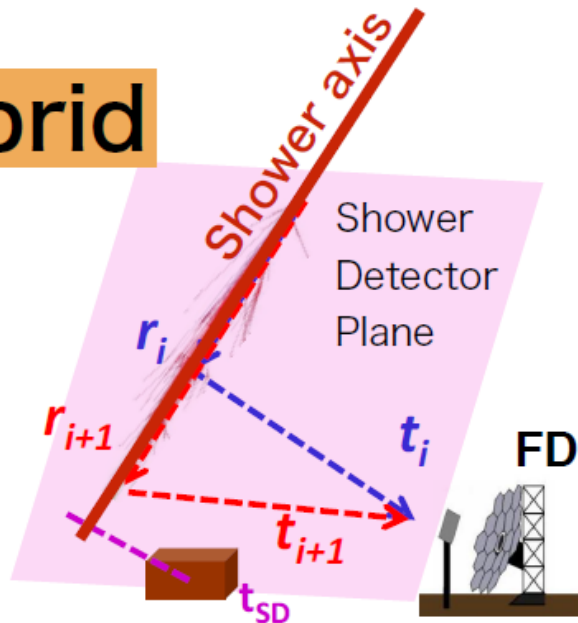
observed images

Stereo



reconstructed shower profiles

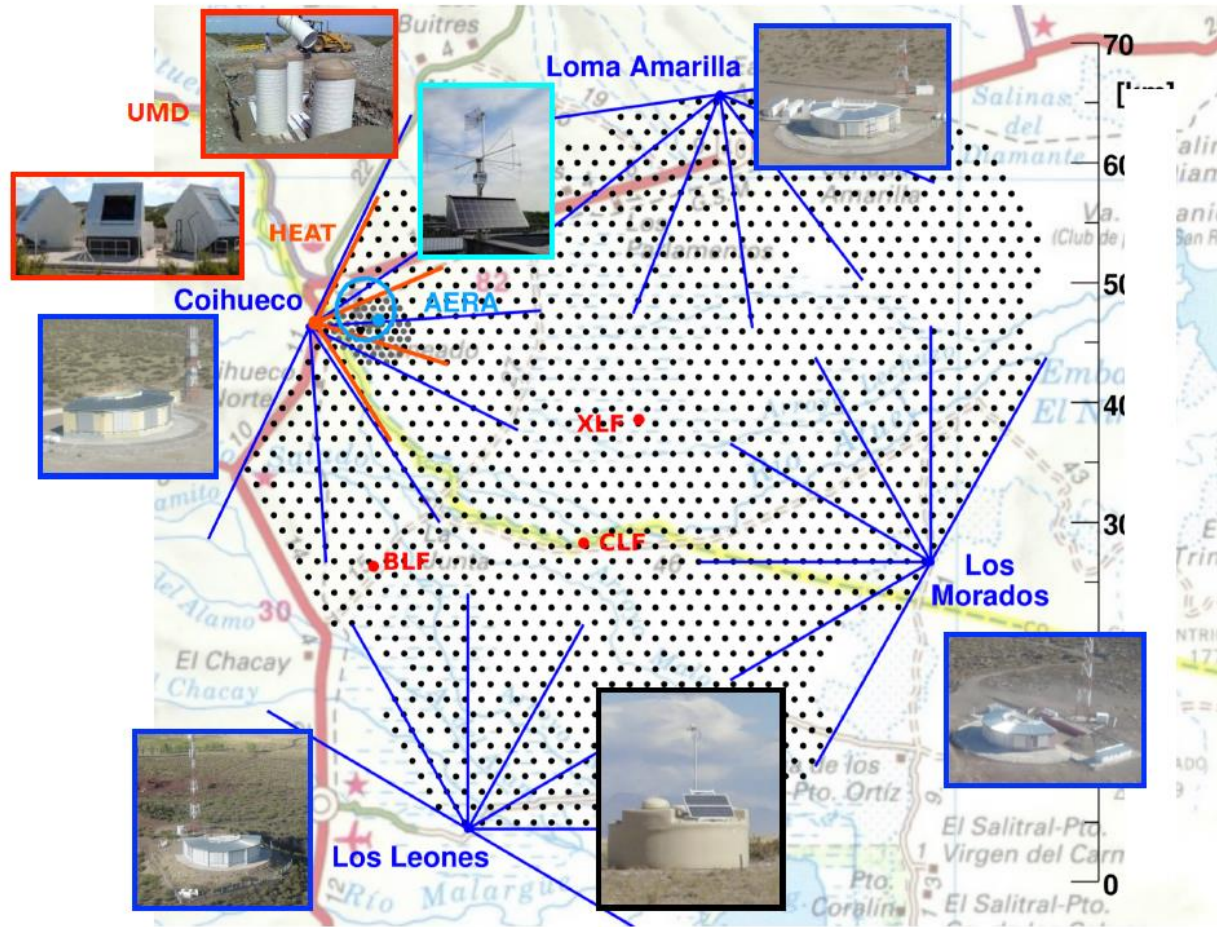
Hybrid



Comparing with MC $\rightarrow X_{max}$
Integration of signals $\rightarrow I_{ry} E$

The Pierre Auger Observatory

TeVPA2019 Dawson



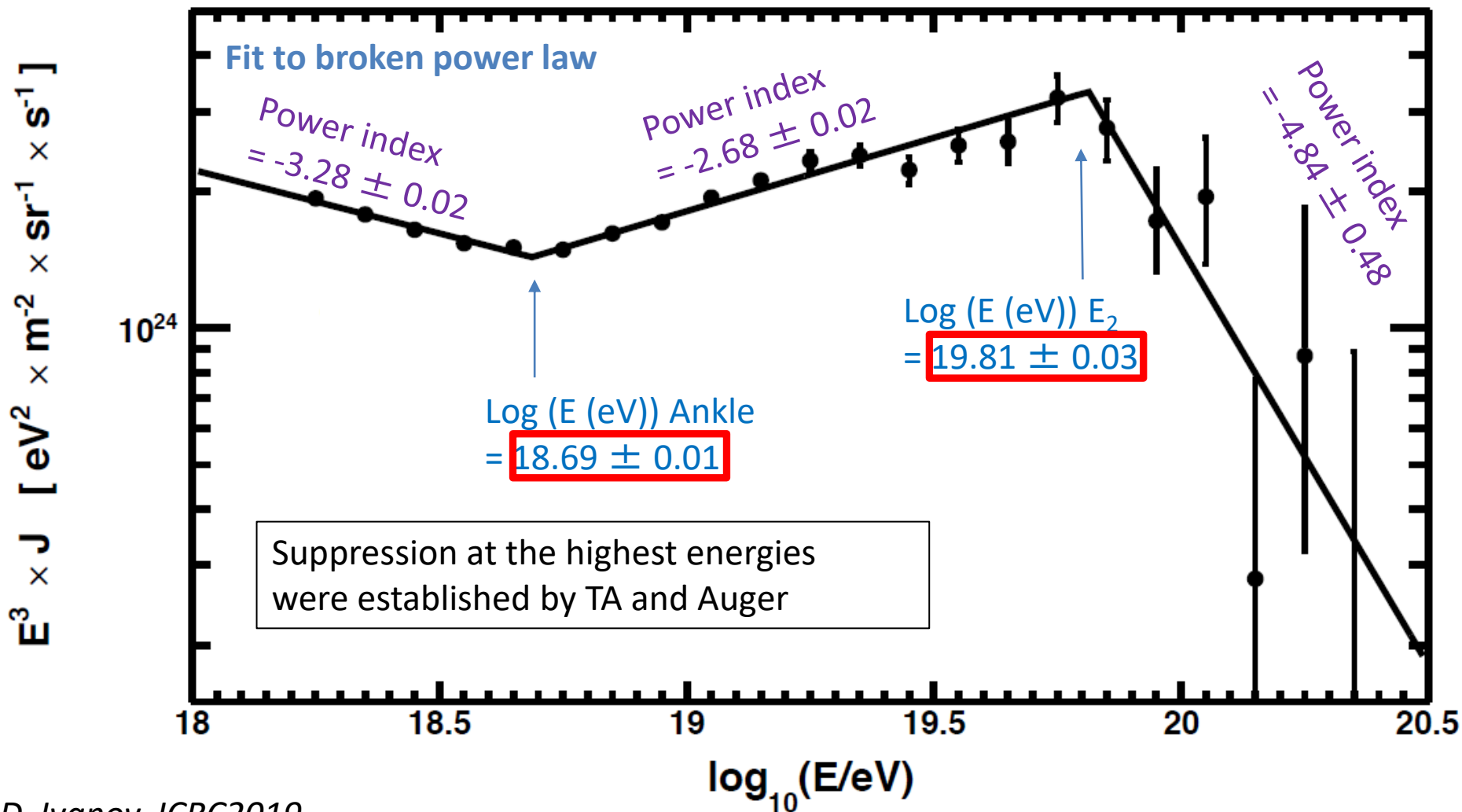
- Water-Cherenkov stations
 - SD1500 : 1600, 1.5 km grid, 3000 km²
 - SD750 : 61, 0.75 km grid, 25 km²
- 4 Fluorescence Sites
 - 24 telescopes, 1-30° FoV
- Underground Muon Detectors
 - 7 in engineering array phase -
 - 61 aside the Infill stations
- HEAT
 - 3 high elevation FD, 30-60° FoV
- AERA radio antennas
 - 153 graded 17 km²
- +Atmospheric monitoring devices
CLF, XLF, Lidars, ...

1.5 km spacing 1600 SDs: cover **~3000 km²**
 4 FD sites
 Operation in a stable mode from 2004

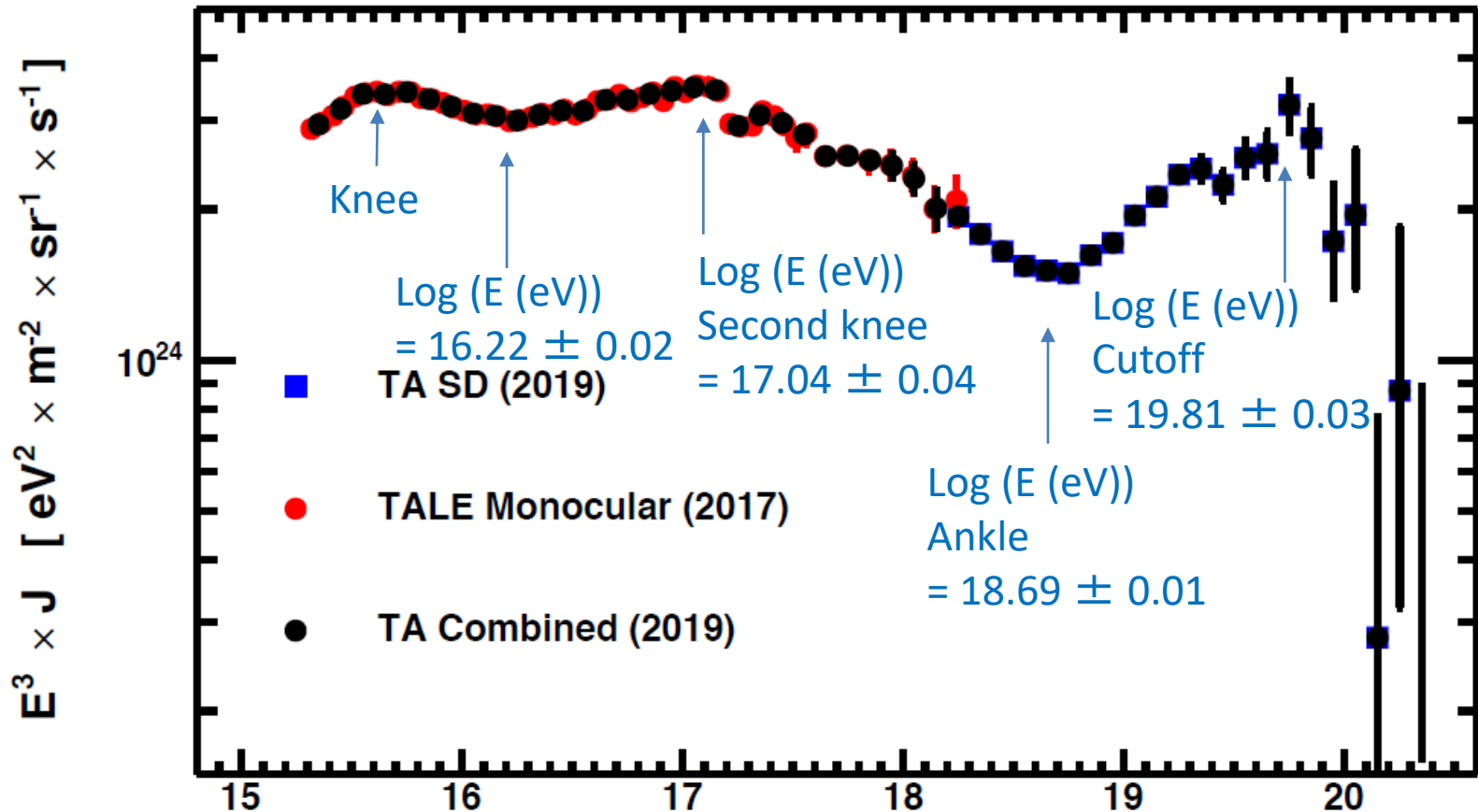
Recent Results

Energy Spectrum with TA SD

TA SD 11 years data



Combined Energy Spectrum with TALE FD Mono



Knee: acceleration limit of protons of galactic sources such as SNRs?
 Second Knee: acceleration limit of irons?

$\log_{10}(E/\text{eV})$

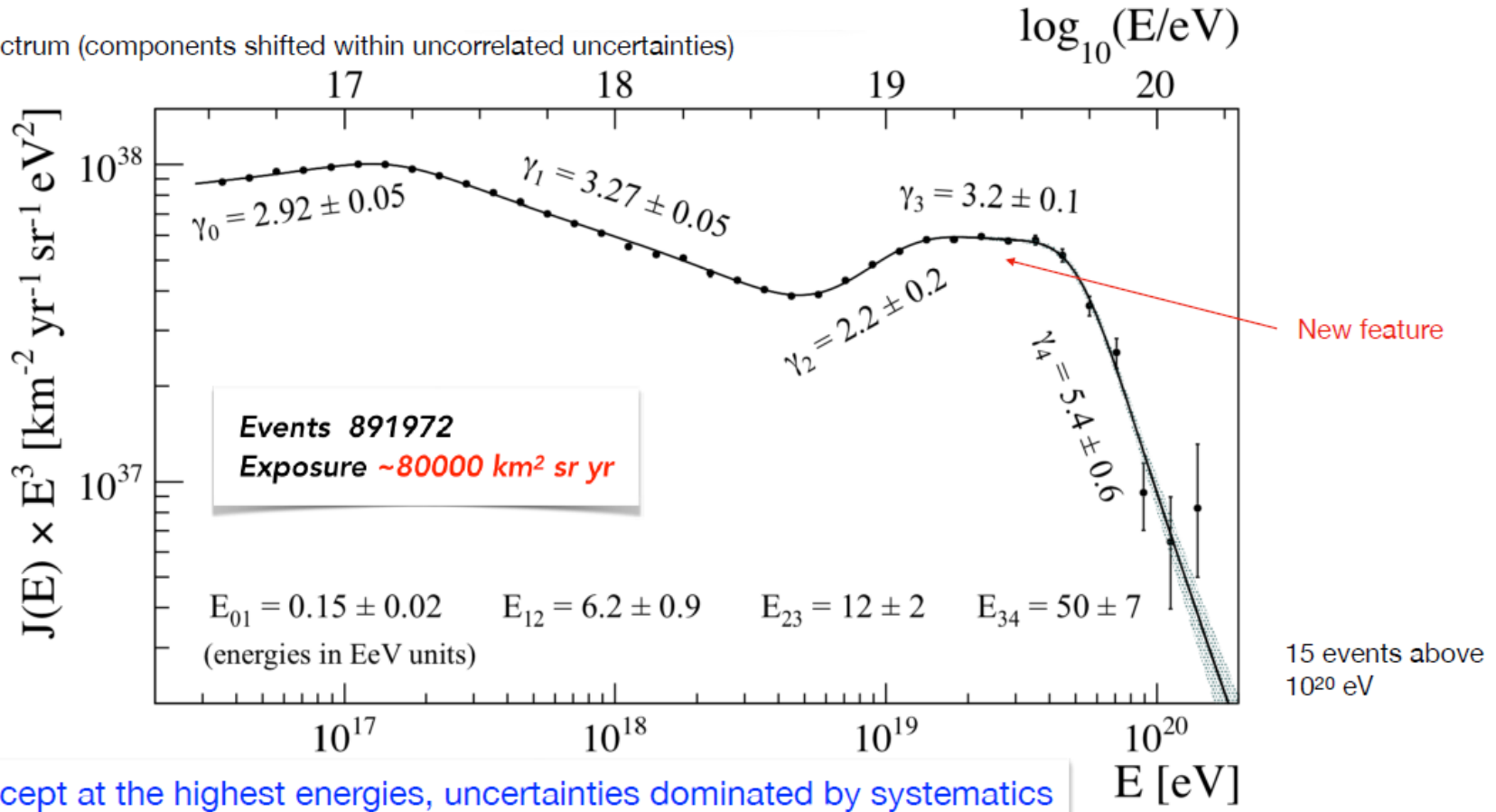
TA can cover wide energy range

Combined TA spectrum using
 22 months TALE FD monocular data +
 11 years TA SD data

Auger Energy Spectrum

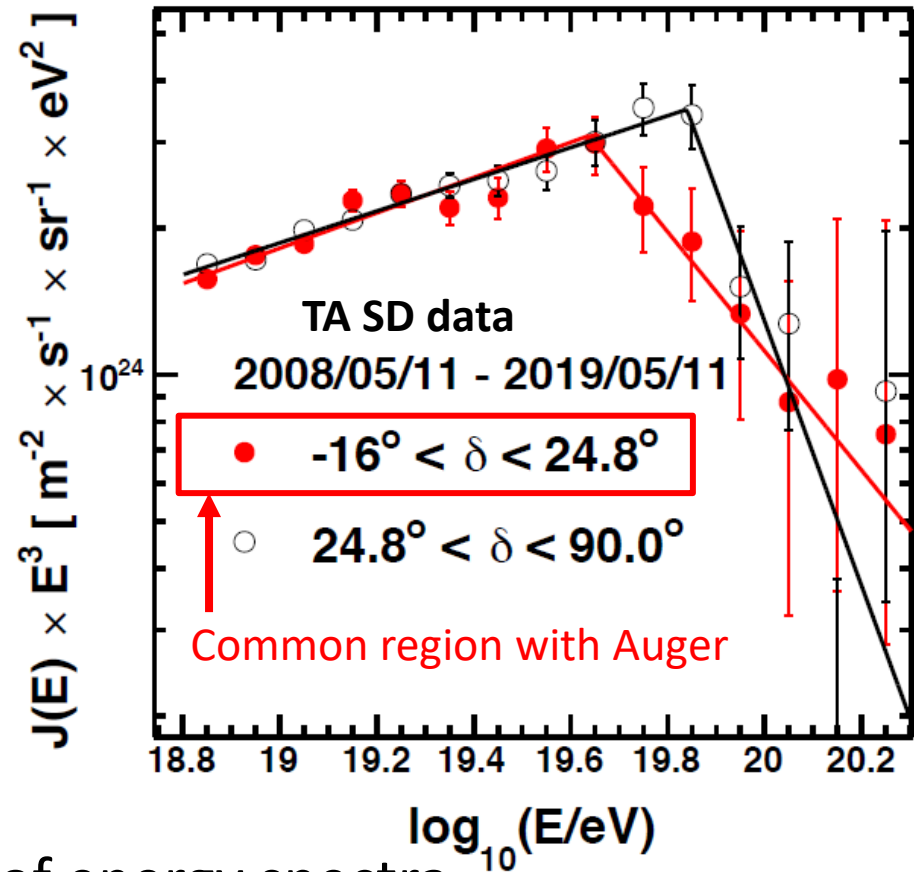
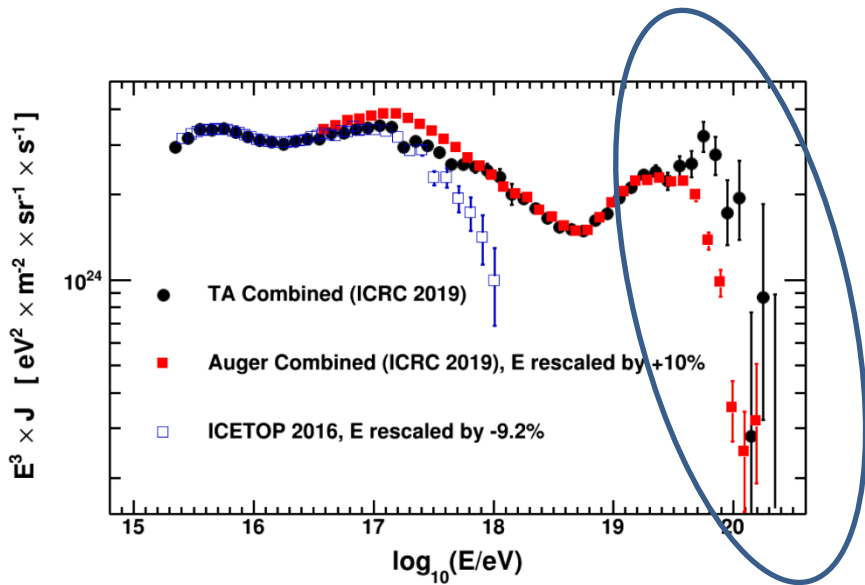
TeVPA2019 Dawson

Combined spectrum (components shifted within uncorrelated uncertainties)



Declination Dependence of Energy Spectrum

D. Ivanov, ICRC2019



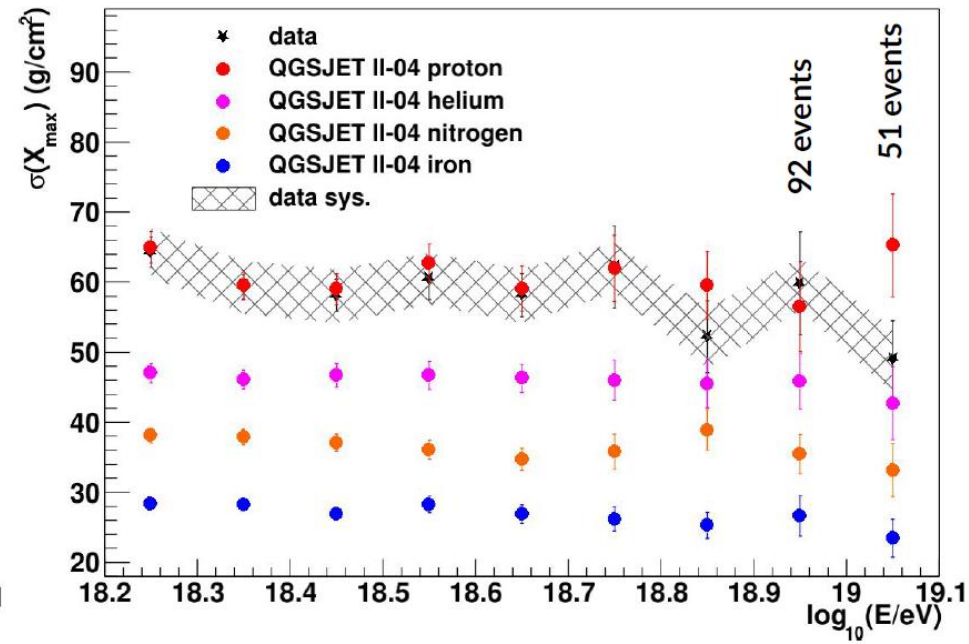
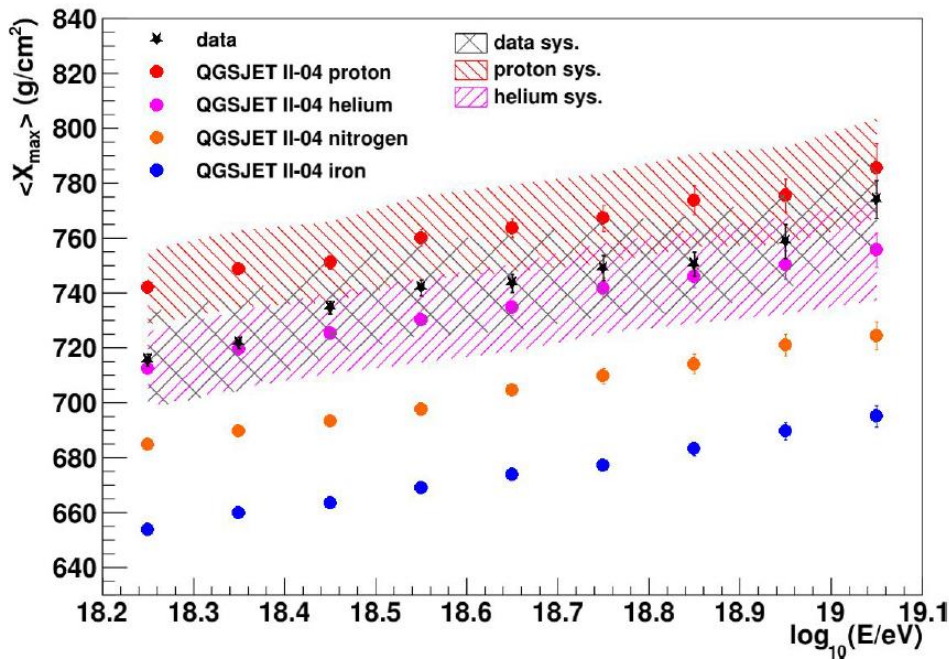
- Difference of the cutoff energies of energy spectra
 - $\log(E/eV) = 19.64 \pm 0.04$ for lower dec. band ($-16^\circ - 24.8^\circ$)
 - $\log(E/eV) = 19.84 \pm 0.02$ for higher dec. band ($24.8^\circ - 90^\circ$)
- The global significance of the difference was estimated to be **4.3 σ**

Composition Analysis with TA SDFD Hybrid Xmax

W. Hanlon, ICRC2019

10 years SD and FD hybrid data
 $\sigma(X_{\max})$

Mean Xmax

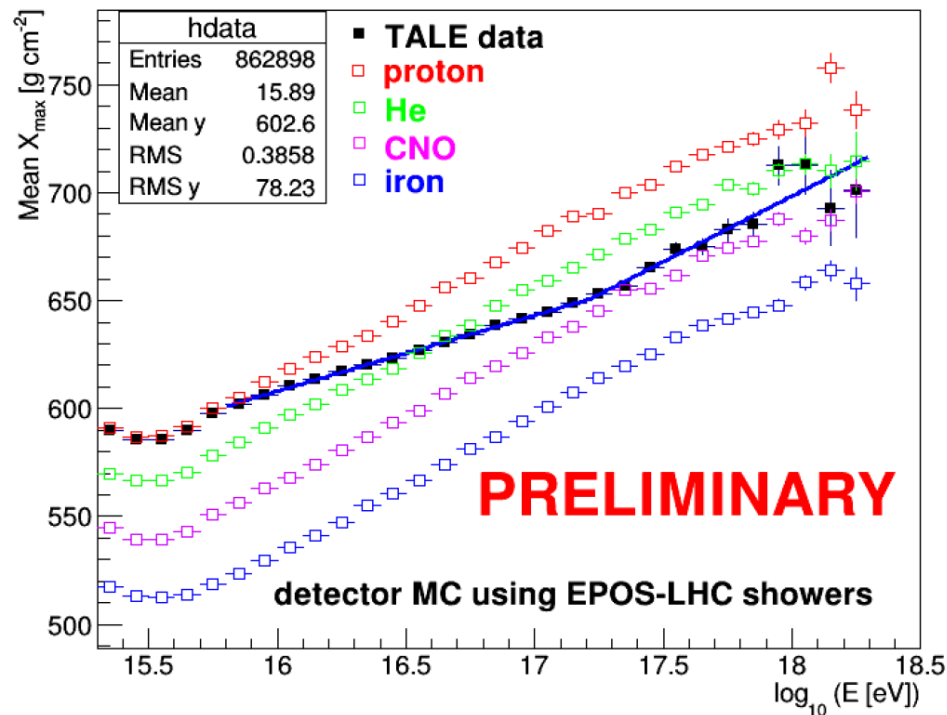


- Energy Range: $10^{18.2} \text{ eV} - 10^{19.1} \text{ eV}$
- 3560 events after the quality cuts
- Systematic uncertainty of $\langle X_{\max} \rangle$: $\pm 17 \text{ g/cm}^2$
- QGSjetII-04 interaction model was compared with the data
→ agreement with light composition
- More events are needed to study highest energies

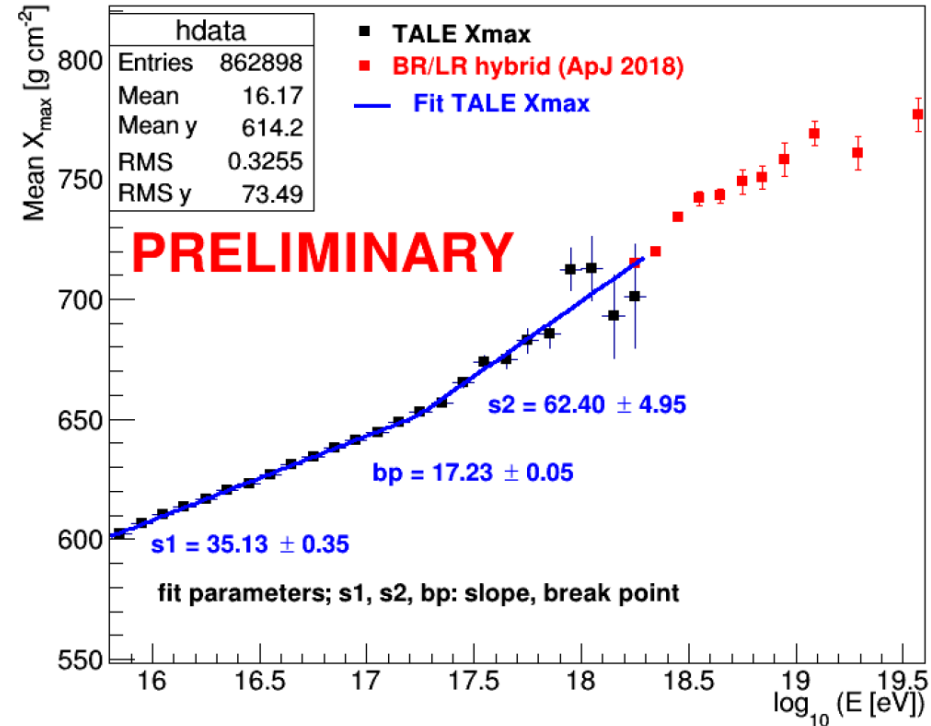
Composition Analysis with TALE FD Mono Xmax

T. Abu-Zayyad, ICRC2019

TALE Reconstructed Shower X_{\max} vs Shower Energy



TALE Mean X_{\max} vs energy

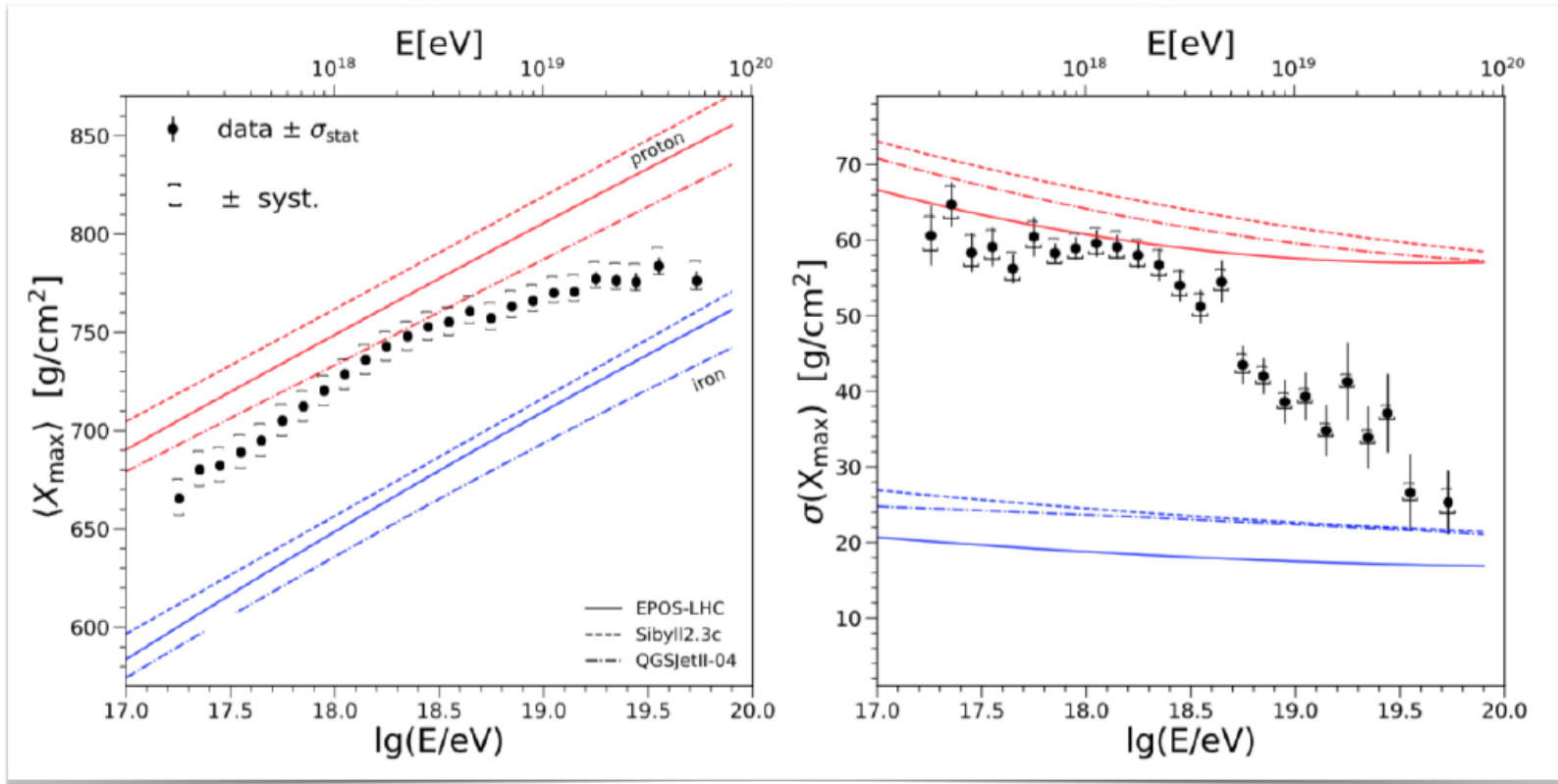


- Jun. 2014 – Nov. 2018 TALE FD mono data
- Energy Range: $10^{15.3} \text{ eV} - 10^{18.3} \text{ eV}$
- Break point $\log(E/\text{eV}) = 17.23 \pm 0.05$

This result is expected to show the transition from galactic CRs to extragalactic CRs

Mean X_{\max} and its fluctuations

TeVPA2019 Dawson



Composition becoming lighter up to $\sim 2 \times 10^{18}$ eV, heavier above this energy

A. Yushkov [Auger Collaboration], ICRC 2019 arXiv:1909.09073

This result is expected to show the transition of compositions of extragalactic CRs at the highest energies.

TA hotspot in the arrival directions of cosmic rays with $E > 57$ EeV

Original hotspot reported in 2014,
from 5 years of data

Ap. J., 790, L21(2014)

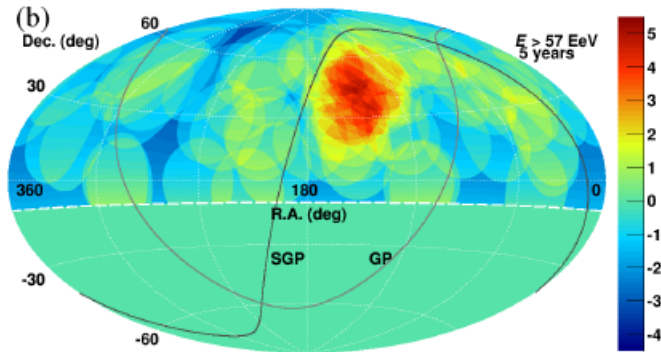
$E > 57$ EeV (Observed 72 events)

20° over-sampling circle

19 events fall in "Hotspot" centered at $(146.7^\circ, 43.2^\circ)$

(Expected = 4.5 events)

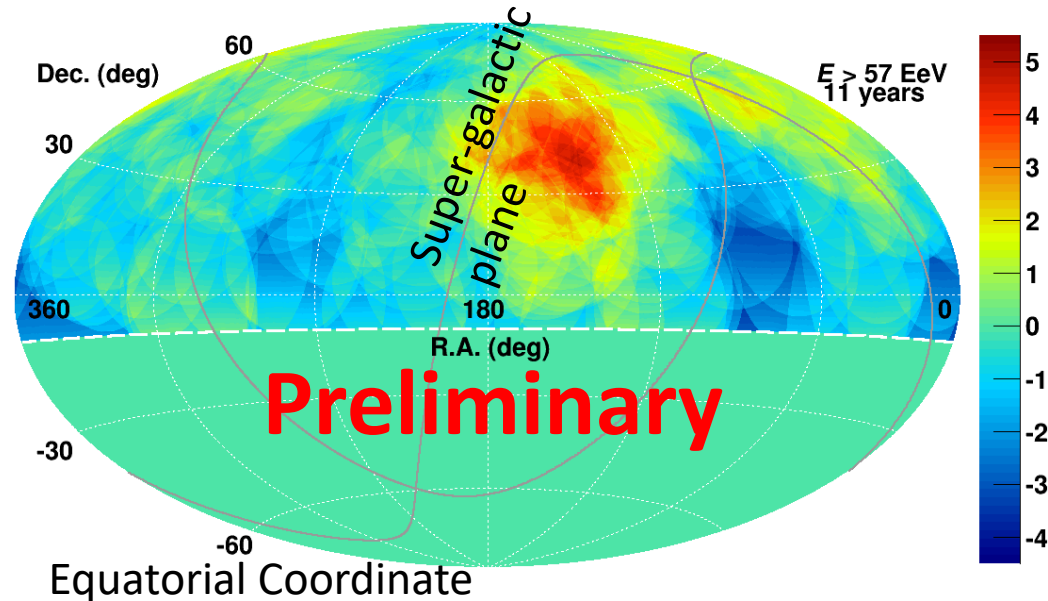
local significance 5.1σ , post trial significance 3.4σ



K. Kawata, ICRC2019

TA SD 11 years data

Significance map from isotropy expectation



$E > 57$ EeV, in total 168 events

38 events fall in Hotspot ($\alpha=144.3^\circ$, $\delta=40.3^\circ$, 25° radius, 22° from SGP), expected=14.2 events

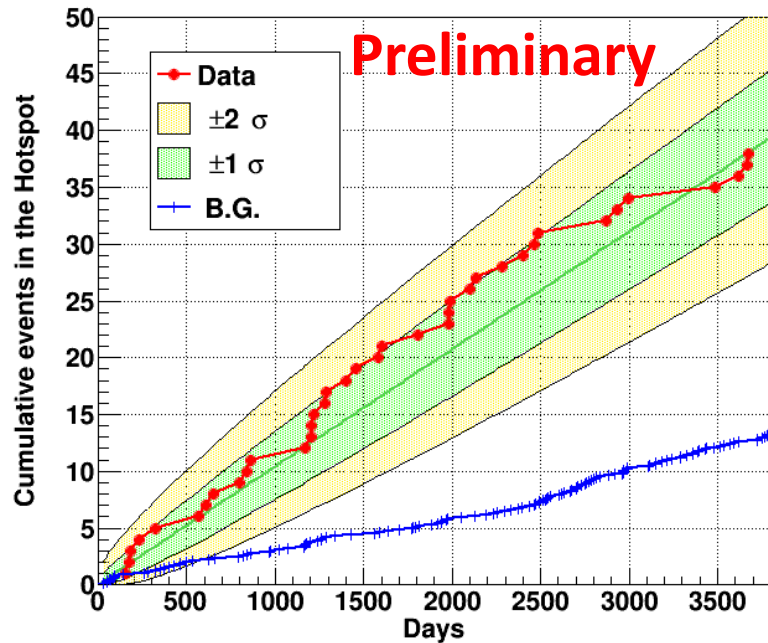
local significance = 5.1σ , chance probability $\rightarrow 2.9\sigma$

25° over-sampling radius shows the highest local significance (scanned 15° to 35° with 5° step)

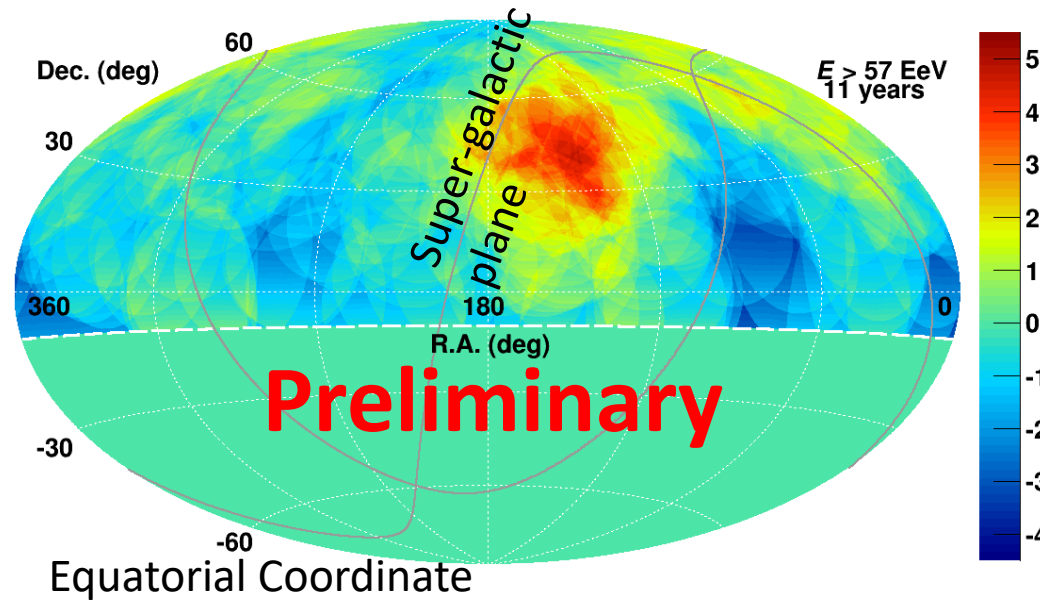
TA hotspot in the arrival directions of cosmic rays with $E > 57 \text{ EeV}$

K. Kawata, ICRC2019

Events within hotspot circle



Significance map from isotropy expectation



The cumulative events inside the hotspot circle (25° -radius circle) defined by the 11-year. The increase rate of the events inside the hotspot circle:

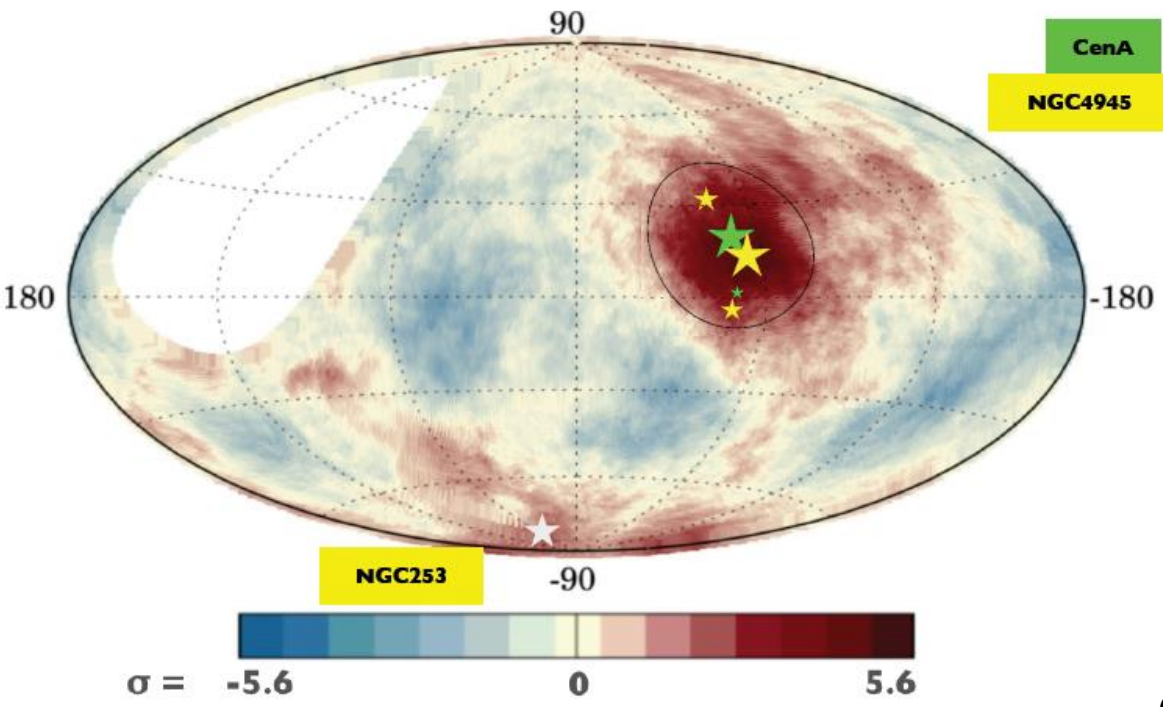
Consistent with the linear increase within $\sim 1\sigma$

Anisotropy in the arrival directions was not discovered before in this energy region. This result would be the implication of the anisotropy.

Auger intermediate-scale anisotropy

TeVPA2019 Dawson

Total SD events with $E > 32 \text{ EeV}$: 2157
Total exposure $101,400 \text{ km}^2 \text{ sr yr}$



Blind search

Scan ranges:
 $32 \text{ EeV} \leq E_{th} \leq 80 \text{ EeV}$ (1 EeV steps)
 $1^\circ \leq \psi \leq 30^\circ$ (1° steps)

Most significant excess for $E > 38 \text{ EeV}$
($\alpha = 202^\circ, \delta = -45^\circ$) $\sim 2^\circ$ from CenA
2.5% post-trial chance probability

Centaurus A

3.9 σ effect (post-trial)
for $E > 37 \text{ EeV}$, 28° window

Cen A (3FHL catalog):
Gal. latitude: 309.5 deg.
Gal. longitude: 19.4 deg.

L. Gaccianiga [Auger Collaboration], ICRC 2019 arXiv:1909.09073

Galactic coordinate

Auger intermediate-scale anisotropy

TeVPA2019 Dawson

γ AGNs

3FHL catalog < 250 Mpc
33 sources (CenA, Fornax A, M87...)
Flux proxy $\phi(>10 \text{ GeV})$

Starburst Galaxies

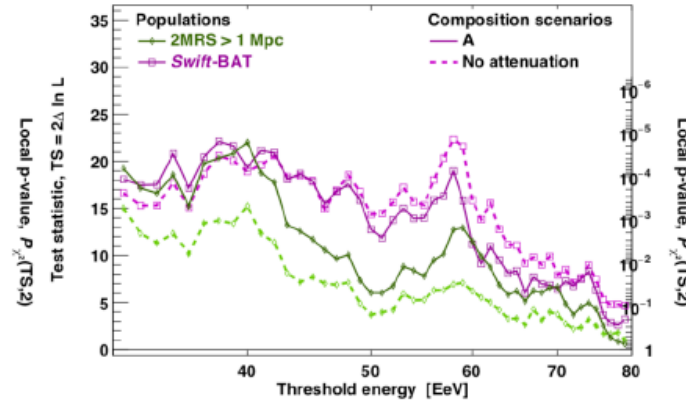
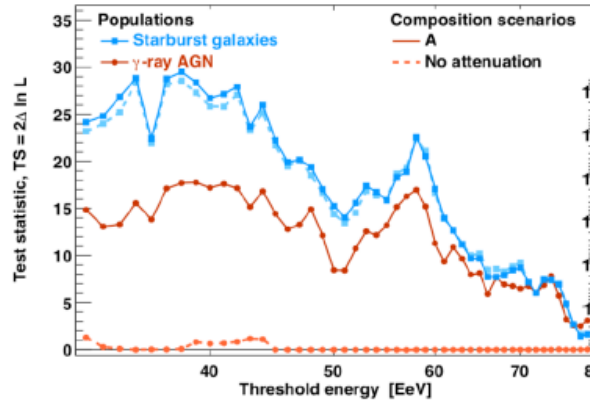
32 sources (Circinus, M82, M83,...)
<250 Mpc
Flux proxy $\phi(>1.4 \text{ GHz}), > 0.3 \text{ Jy}$

Swift-BAT

>300 radio loud and quiet sources
<250 Mpc
 $\phi > 13.4 \cdot 10^{-12} \text{ erg cm}^{-2} \text{ s}^{-1}$

2MRS

$\sim 10^4$ sources with $D > 1 \text{ Mpc}$
<250 Mpc
Flux proxy K-band flux.



Likelihood analysis $TS = 2 \text{Log} [L(\psi, f_{anis}) / L(f_{anis} = 0)]$



Catalog	E_{th}	TS	Local p-value	post-trial	f_{anis}	θ
Starburst	38 EeV	29.5	4×10^{-7}	4.5 σ	$11^{+5}_{-4}\%$	$15^{+5}_{-4}^\circ$
γ -AGN	39 EeV	17.8	1×10^{-4}	3.1 σ	$6^{+4}_{-3}\%$	$14^{+6}_{-4}^\circ$
Swift-BAT	38 EeV	22.2	2×10^{-5}	3.6 σ	$8^{+4}_{-3}\%$	$15^{+6}_{-4}^\circ$
2MRS	40 EeV	22.0	2×10^{-5}	3.6 σ	$19^{+10}_{-7}\%$	$15^{+7}_{-4}^\circ$

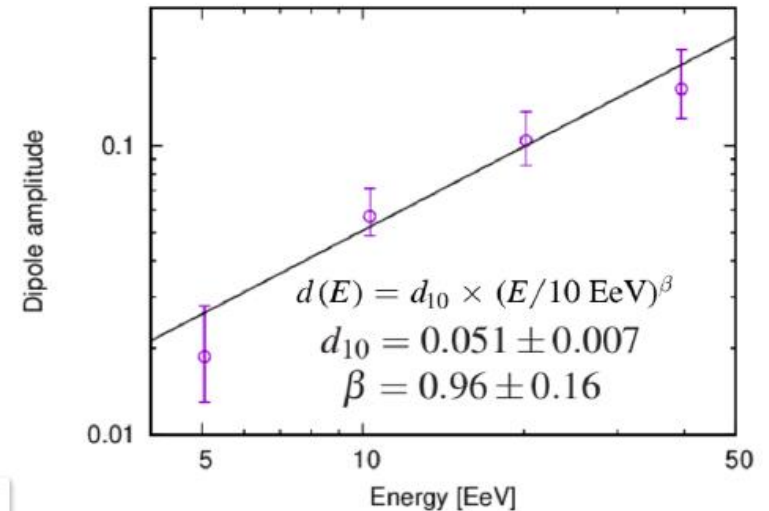
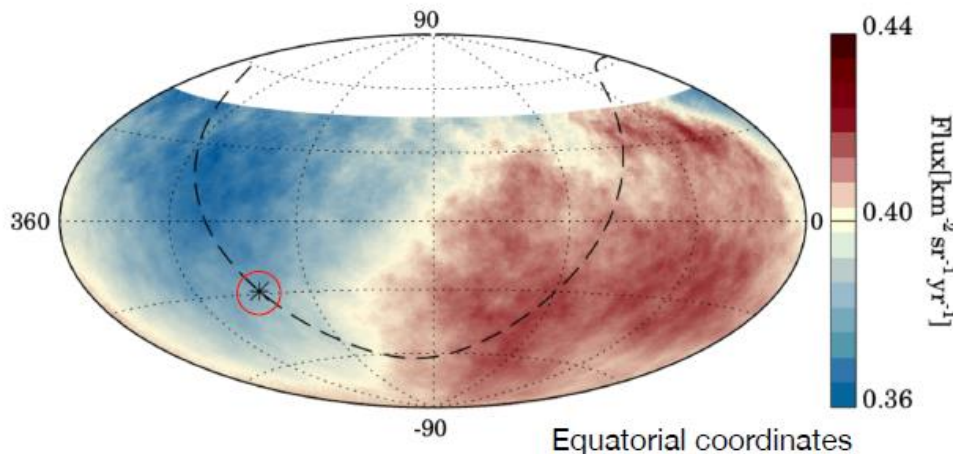
(given source smearing, clearly some overlap between catalogs)

Auger large-scale anisotropy

TeVPA2019 Dawson

Exposure > 92000 km² sr yr
for events with $\theta < 80^\circ$

Energy [EeV]	N	d_\perp	d_z	d	α_d [°]	δ_d [°]	
interval median							
4 - 8	5.0	88,317	$0.010^{+0.007}_{-0.004}$	-0.016 ± 0.009	$0.019^{+0.009}_{-0.006}$	70 ± 34	-57^{+24}_{-20}
≥ 8	11.5	36,924	$0.060^{+0.010}_{-0.009}$	-0.028 ± 0.014	$0.066^{+0.012}_{-0.008}$	98 ± 9	-25 ± 11



3D dipole above 8×10^{18} eV at $(\alpha, \delta) = (98^\circ, -25^\circ)$: $(6.6^{+1.2}_{-0.8})\%$
Amplitude increasing with energy

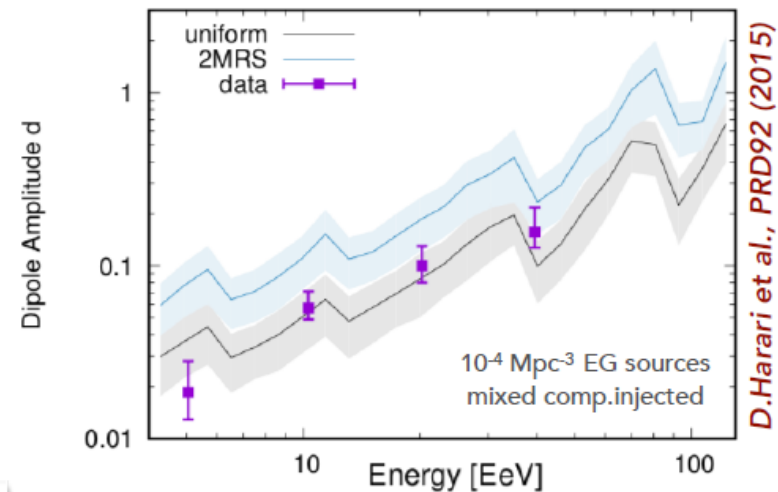
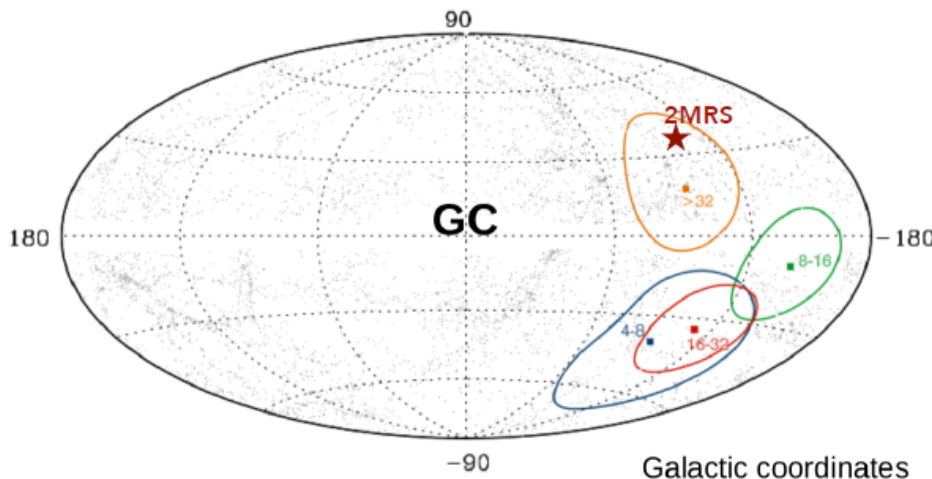
A. Aab et al. [Auger Collaboration], Science **357** 1266 (2017); E. Roulet [Auger Collaboration], ICRC 2019 arXiv:1909.09073

Dipole $E > 8$ EeV was discovered at **$> 5.2\sigma$** significance level in 2017
Energy dependence was also discovered at **5.1σ** significance in 2019

Large-scale anisotropy

Energy [EeV]	N	d_{\perp}	d_z	d	$\alpha_d [^{\circ}]$	$\delta_d [^{\circ}]$	
interval median							
4 - 8	5.0	88,317	$0.010^{+0.007}_{-0.004}$	-0.016 ± 0.009	$0.019^{+0.009}_{-0.006}$	70 ± 34	-57^{+24}_{-20}
≥ 8	11.5	36,924	$0.060^{+0.010}_{-0.009}$	-0.028 ± 0.014	$0.066^{+0.012}_{-0.008}$	98 ± 9	-25 ± 11

Exposure $> 92000 \text{ km}^2 \text{ sr yr}$
for events with $\theta < 80^{\circ}$



3D dipole above $8 \times 10^{18} \text{ eV}$ at $(\alpha, \delta) = (98^{\circ}, -25^{\circ})$: $(6.6^{+1.2}_{-0.8})\%$
Amplitude increasing with energy

A. Aab et al. [Auger Collaboration], Science **357** 1266 (2017); E. Roulet [Auger Collaboration], ICRC 2019 arXiv:1909.09073

Anisotropy is expected to be come from nearby extragalactic sources by comparing with the distribution of nearby galaxies.

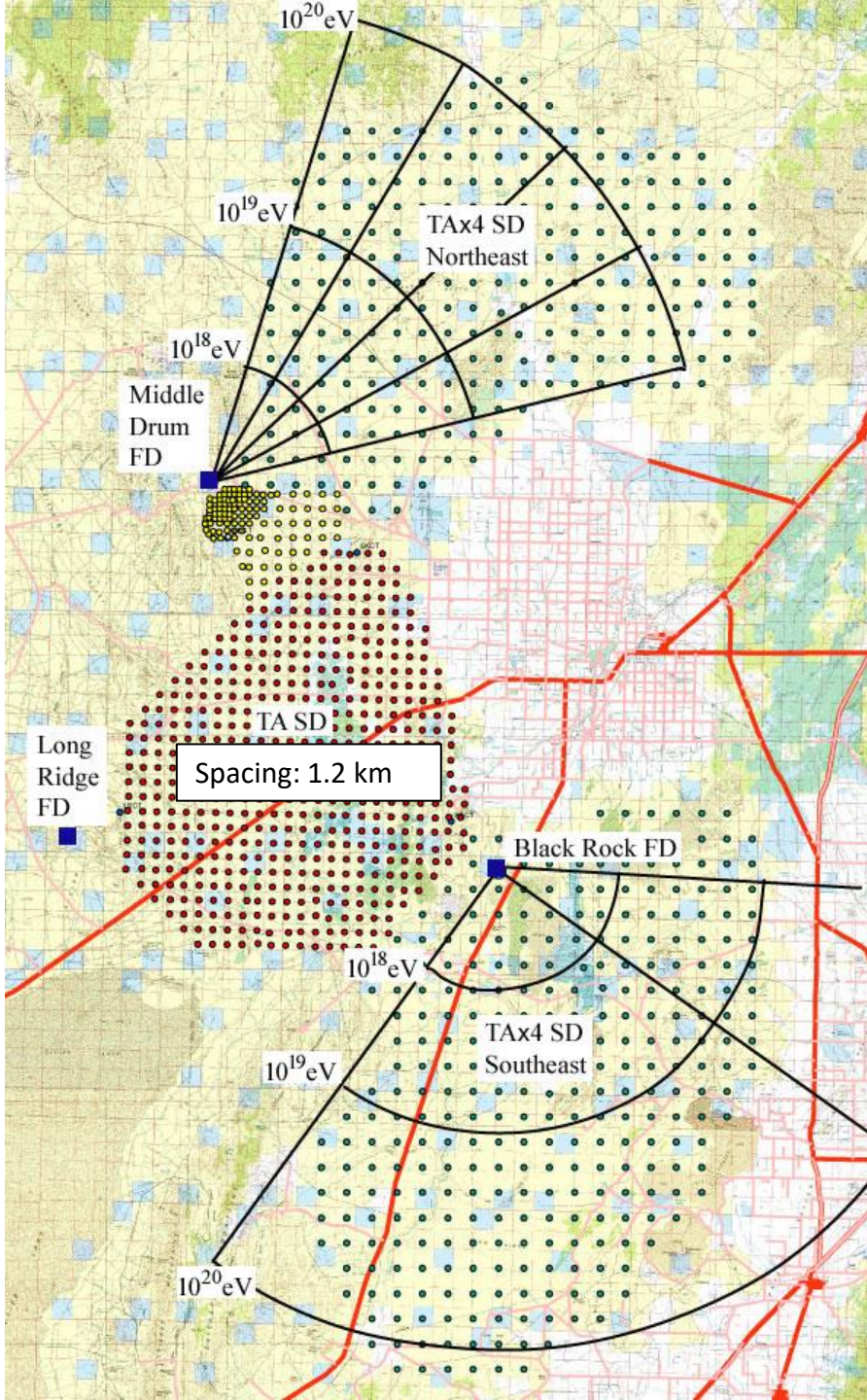
Summary

- Energy Spectrum
 - TA: **Declination dependence** was claimed at **4.3 σ** in the energy spectrum
 - Auger: **New flattening feature** was found in the spectral shape at the highest energies
- Composition
 - TA SD and FD hybrid: consistent **with light composition** with $\log(E/\text{eV}) > \mathbf{18.2}$ and $\log(E/\text{eV}) < \mathbf{19.1}$
 - Auger: composition becoming lighter up to $2 \cdot 10^{18}$ eV and heavier than this energy
- Intermediate-scale anisotropy
 - TA: **2.9 σ hotspot**, oversampling radius: 25° $E > \mathbf{57}$ EeV
 - Auger: **4.5 σ correlation with starburst galaxies**, oversampling radius: 15° $E > \mathbf{38}$ EeV
- Large-scale anisotropy
 - Auger: dipole was detected in **>5.2 σ** , $E > 8$ EeV in 2017
- **Implications of anisotropy are showing up from both TA and Auger at the highest energies.**

Ongoing Upgrades

The TAx4 experiment

ICRC2019
Kido



To study more about the highest energies and examine the implications obtained by TA

500 new SDs with 2.08 km spacing

$E > 57$ EeV:

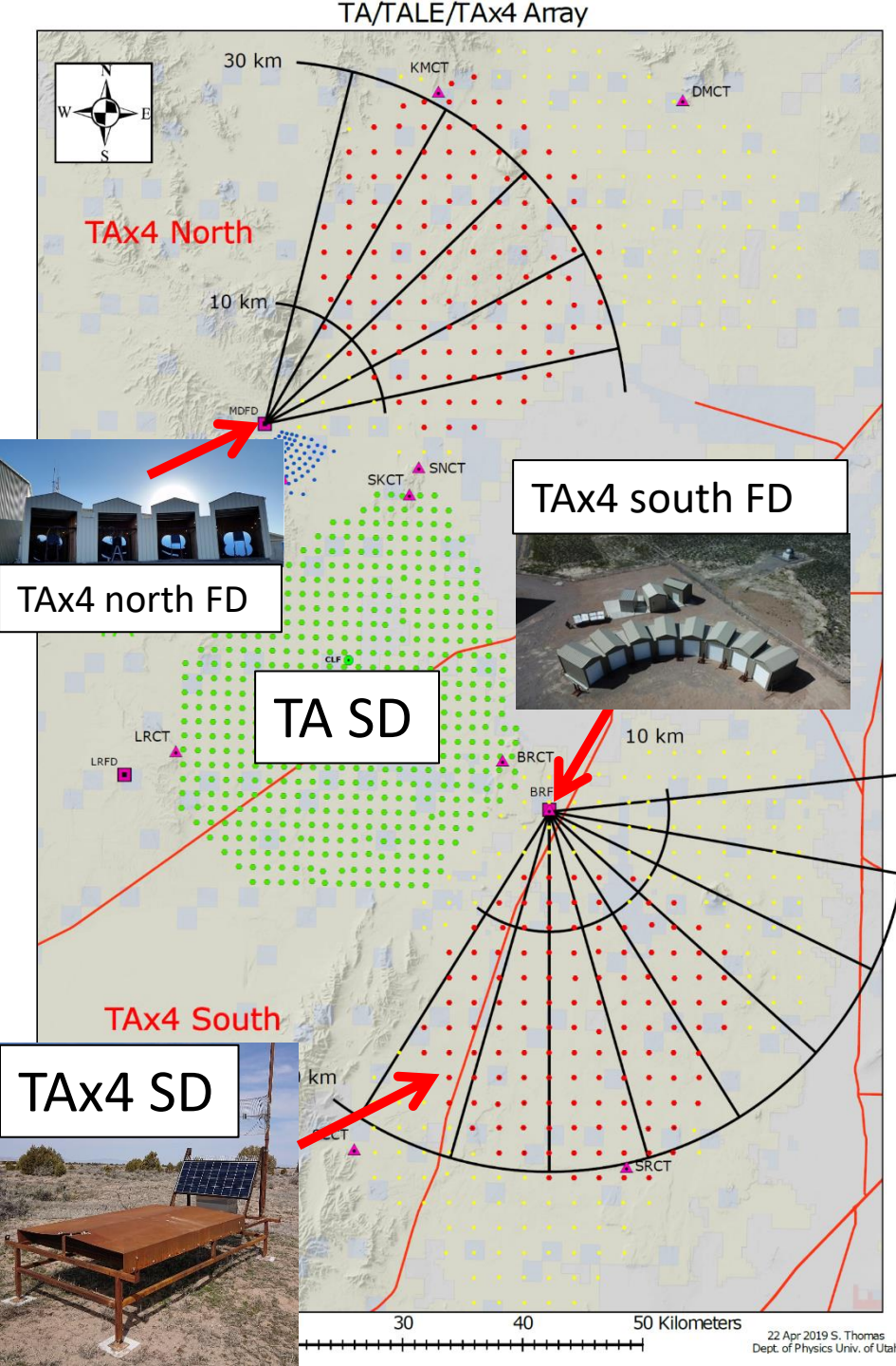
- Reconstruction efficiency $> 95\%$
- Angular resolution: 2.2°
- Energy resolution: $\sim 25\%$

and TA SDs cover

$4 \times$ TA SD detection area (~ 3000 km 2)

2 new Fluorescence Detector (FD) stations (4+8 HiRes Telescopes)

Deployed SDs and Communication Towers



- **More than half of SDs (257 SDs)** were deployed on 19 Feb. – 12 Mar. 2019.
- Locations of SDs were decided to optimize hybrid events above 10 EeV and consider practical conditions of wireless communications
→ **$\sim 3 \times$ TA SDFD** equivalent hybrid events will be collected

Construction of TAx4 SDs



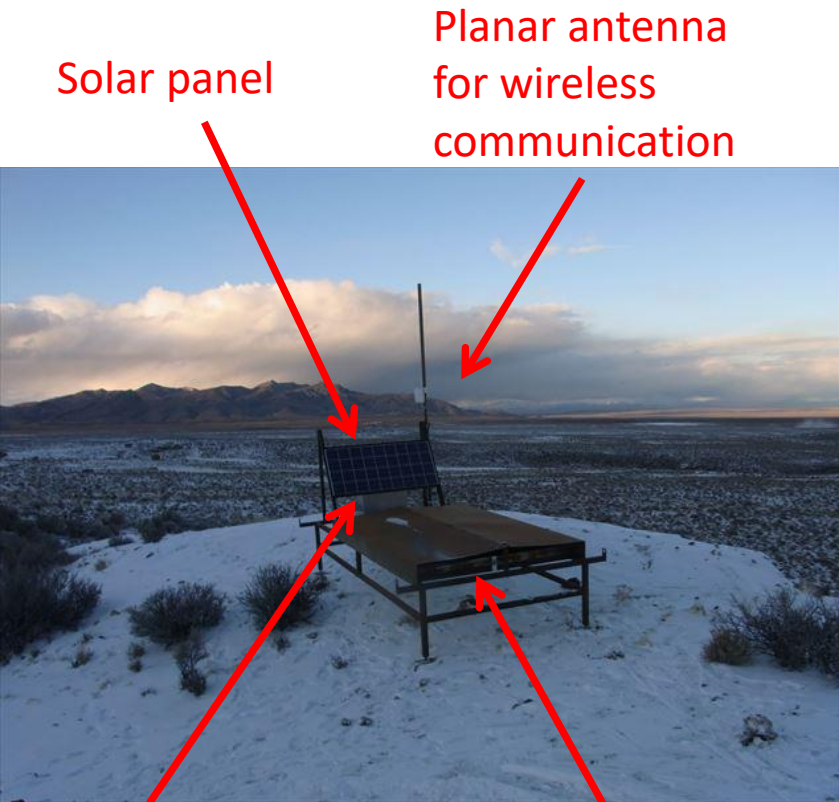
Deployment of Assembled SDs

<https://www.flickr.com/photos/142880279@N06/albums/72157689940402503>

Helicopter for the transportation of SDs



Design of SDs

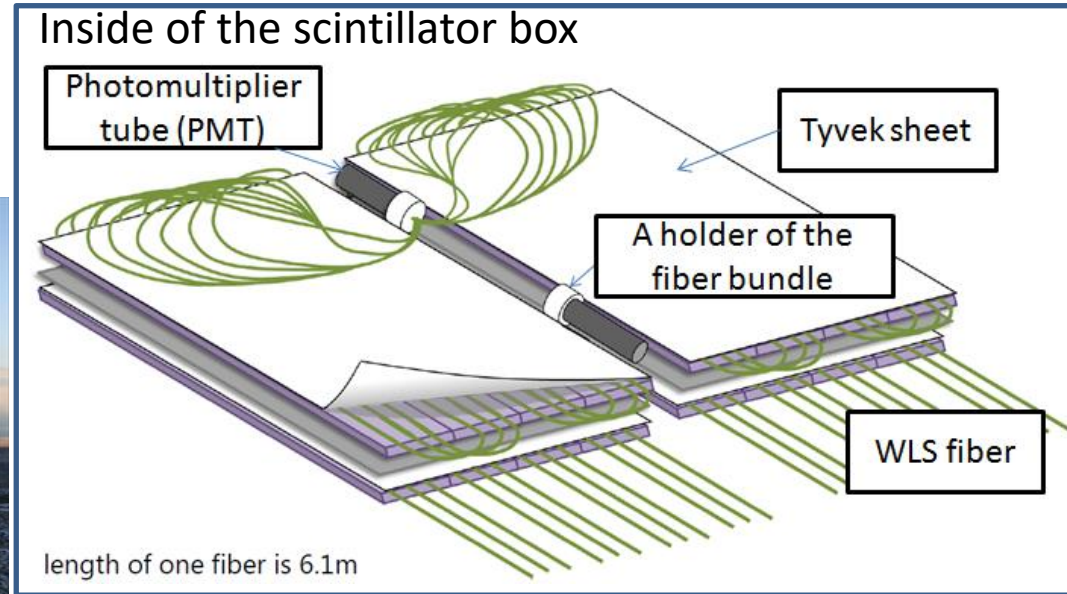


Solar panel

Planar antenna
for wireless
communication

Scintillator box

Stainless steel box
for the electronics
and a battery



- **2 layers 3 m² 1.2 cm thick plastic scintillators**
→ Calibration of signals using single muons
- DAQ with 2.4 GHz wireless communication

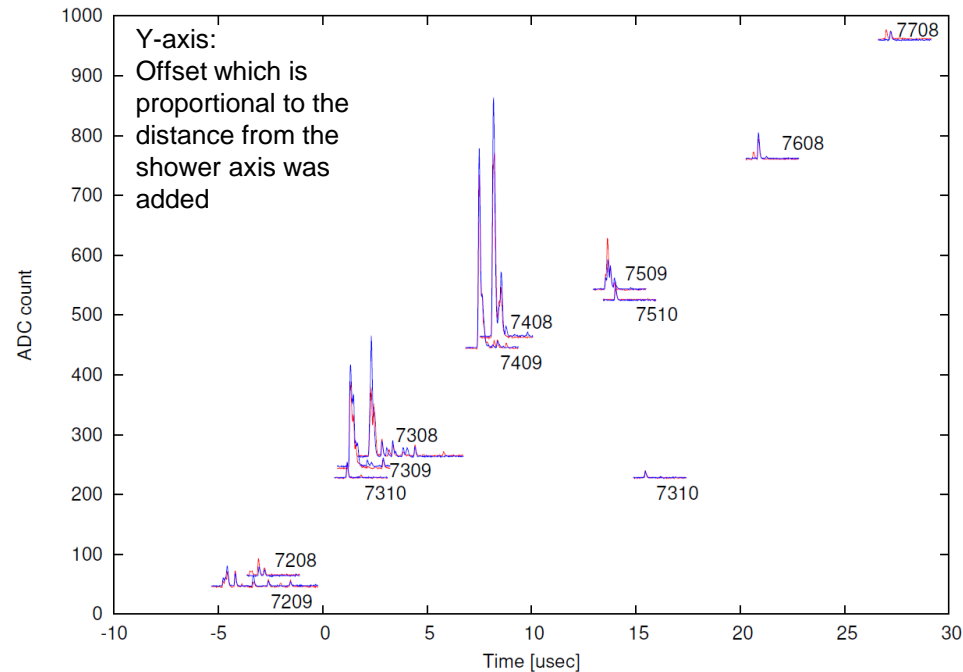
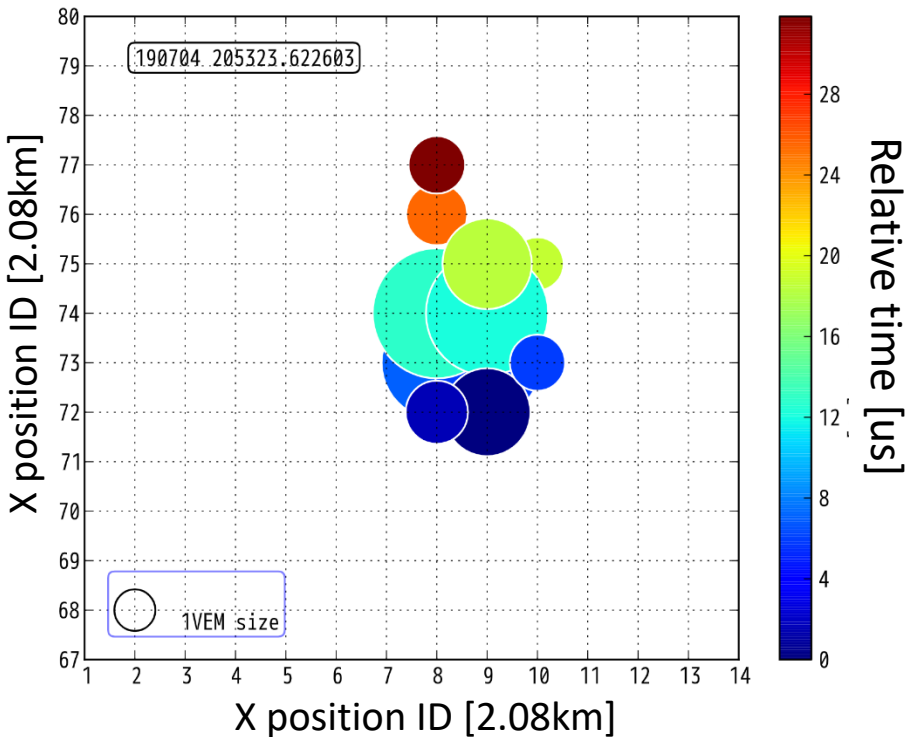
PMT and arrangement of WLF fibers (**33%** of TA SDs) was changed from TA SD for the cost reduction

Single peak: **21 p.e.** in average (**~ TA SDs**)

Non-uniformity: **< 15 %** (**~1/2 x TA SDs**)

Pulse linearity: **50 mA** (**~2 x TA SDs**)

Cosmic Ray Event ($E > 57 \text{ EeV}$)



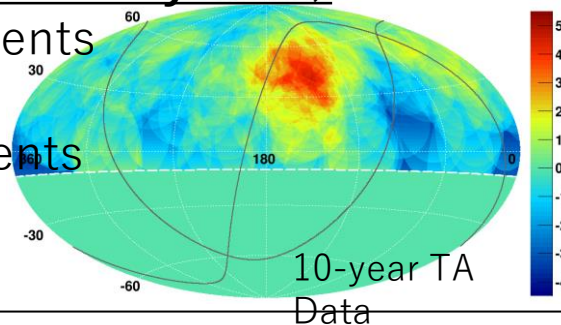
We started stable observation

SD: from 2019 Nov. , FD(north): from 2018 Jun. FD(south): from 2020 Sep.

Expectation of Hotspot in next 5 years

Hypothesis (10-yr observation from May 2008):

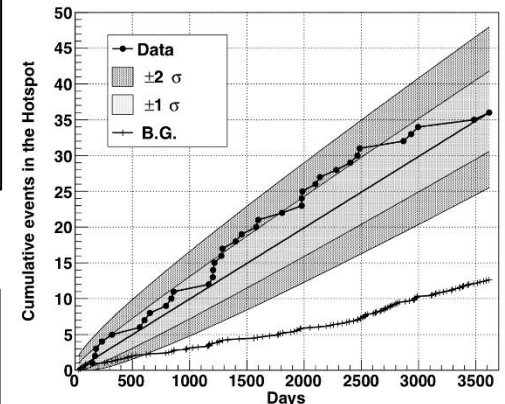
- Total # of events: 157 events
→ 15.7 events/yr
- Hotspot # of events: 36 events
(25° radius circle)
→ 3.6 events/yr



↓ Simple extrapolation

Expectation (as of May 2025): 12-yr TA + 5-yr TA \times 2.5 = 24.5-year TA

- Total # of events: 384 events
- Hotspot # of events: 88 events (25° radius circle)
→ Local Li-Ma Significance: 7.8 σ
Global Significance: 7.8 σ - 2 σ = ~6 σ



Auger upgrade (AugerPrime)



4 m² thickness: 1cm
plastic scintillator

Auger water tank

ICRC 2015
Engel #686

SD statistics $\sim 10 \times$ FD statistics

Plastic scintillator is added to the water tank SD:

measure electromagnetic component, muon component

→ R&D of the method to determine

the mass composition of cosmic rays using **only SD**

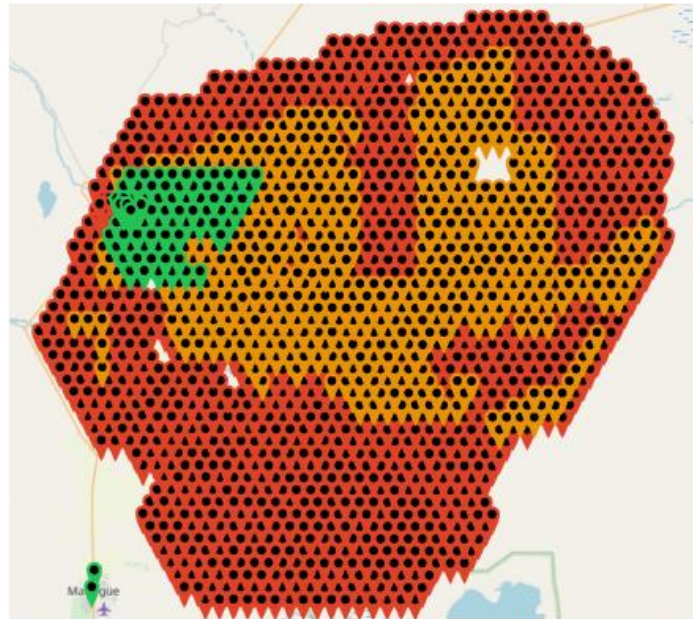
→ **Mass composition at the highest energies with large statistics**

(operation: 2018-)

AugerPrime - deployment underway

Mass-composition information for all events, including the very highest energies.

- Engineering array (12 stations) since 2016, scintillator (SSD), new electronics (faster sampling, increased dynamic range)
- Pre-production SSD array (80 stations) since March 2019.
- 559 SSD stations installed up to now (Nov 2019)
- Underground muon detector (UMD) construction continues
- New: 3000 km² radio detector



November 17, 2019



Water-Cherenkov detector (WCD) with new surface scintillator detector (SSD) and new radio antenna.

Interpretation of the Experimental Data

Sources – Generic model

Generic assumptions

- Choices following Auger Combined Fit
...extended to source evolution

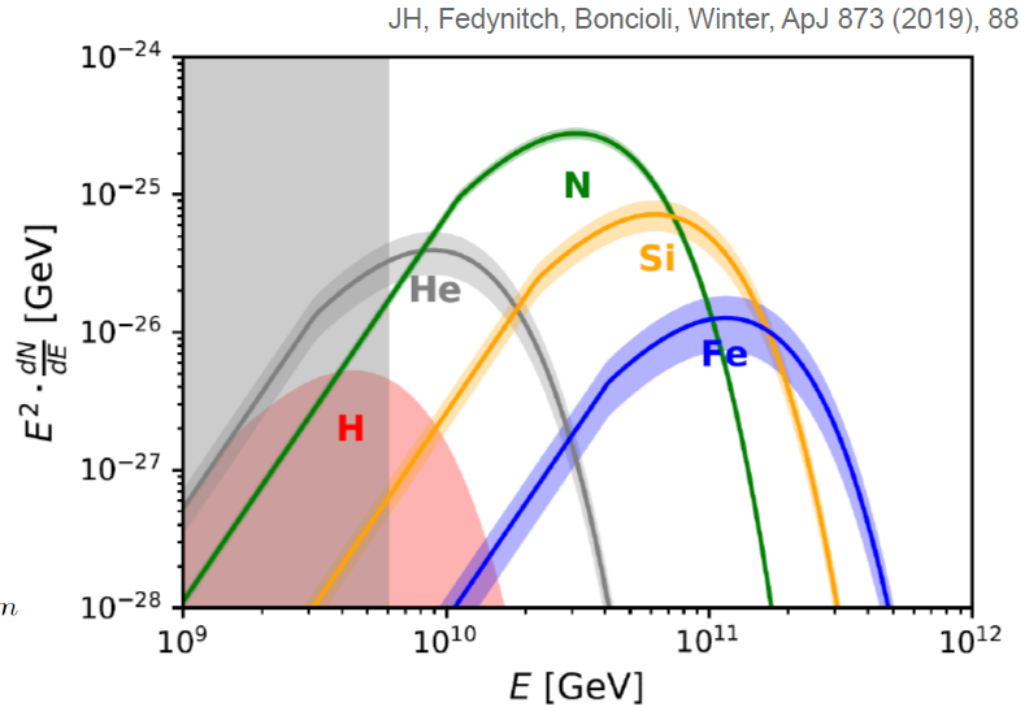
Auger Collaboration, JCAP04(2017)038

- Only five injection elements:
H, He, N, Si, Fe

- Simple Power-law with
rigidity dependent cut-off

$$J_A(E) = \mathcal{J}_A \left(\frac{E}{10^9 \text{ GeV}} \right)^{-\gamma} \times f_{\text{cut}}(E, Z_A, R_{\text{max}}) \times n_{\text{evol}}(z)$$

- Source evolution locally as $n_{\text{evol}}(z) = (1 + z)^m$



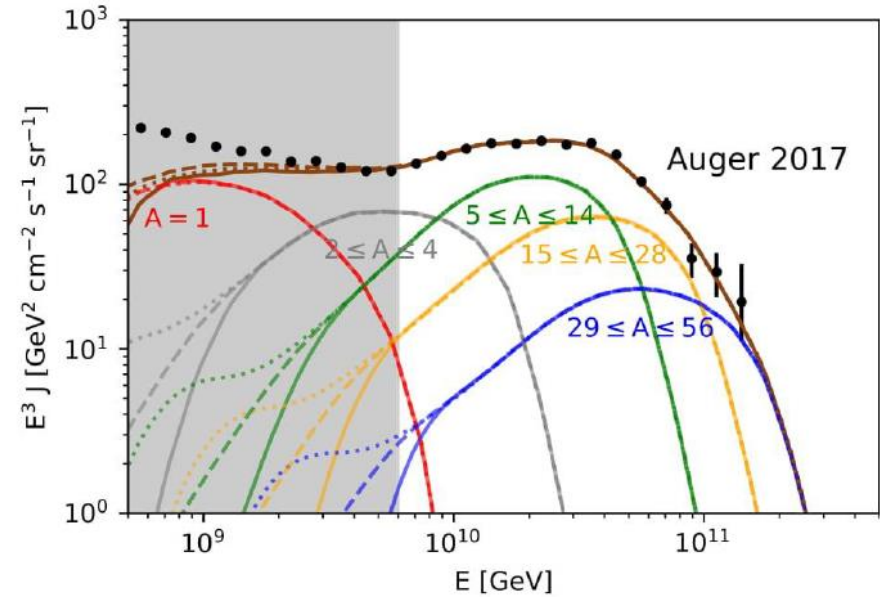
Total of 8 free parameters

→ Fit observed energy spectrum and X_{max}

Results: Best fit spectrum

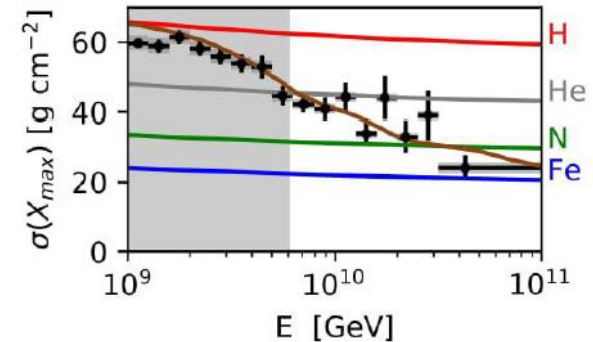
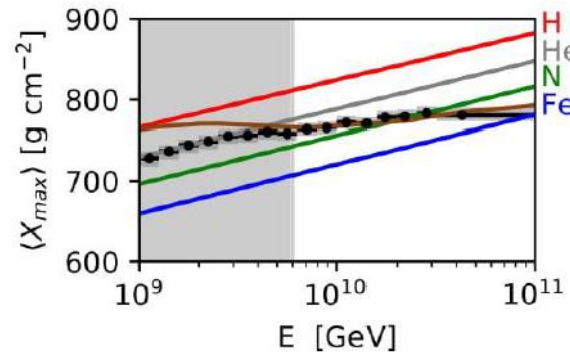
For combination Talys – Sibyll 2.3

- Fit mainly sensitive to envelope of cutoffs
- Fit-range insensitive above $z = 1!$
- Composition below ankle proton dominated (by construction) ...
- ... additional heavy component needed (galactic)



JH, Fedynitch, Boncioli, Winter, ApJ 873 (2019), 88

	best fit (●)		
γ	$-0.80^{+0.27}_{-0.23}$		
R_{\max} (GV)	$(1.6 \pm 0.2) \cdot 10^9$		
m	$4.2^{+0.4}_{-0.6}$		
δE	$0.14^{+0.00}_{-0.03}$		
$f_A(\%)$	H	He	N
	$0.0^{+42.6}_{-0.0}$	$82.0^{+3.8}_{-6.4}$	$17.3^{+1.0}_{-1.1}$
	Si	Fe	
	0.6 ± 0.1	$(2.0 \pm 0.8) \cdot 10^{-2}$	
$I_A^9(\%)$	H	He	N
	$0.0^{+1.2}_{-0.0}$	$9.8^{+2.8}_{-2.9}$	$69.2^{+1.5}_{-1.6}$
	Si	Fe	
	$17.9^{+3.2}_{-3.5}$	$3.2^{+1.2}_{-1.3}$	
χ^2 / dof	27.0 / 21		



Model dependence of the Fit

Compared in $\gamma - m$ space

Disintegration model

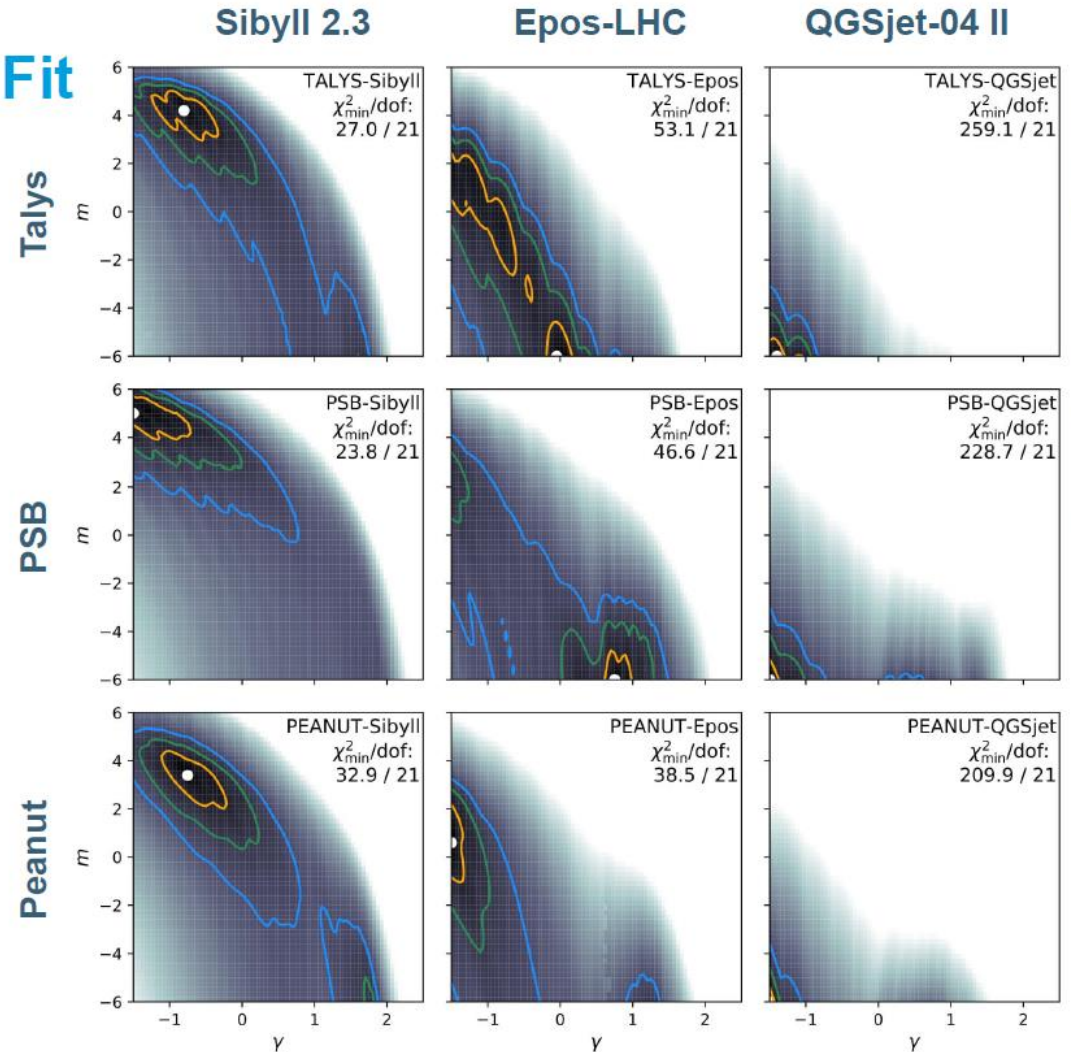
- Qualitatively similar fits
- PSB: **Lighter** injection
- Peanut/Talys: **Heavier** injection

Shower model

- Epos-LHC: Two distinct minima **avoids disintegration**
- Sibyll 2.3: Larger allowed space **prefers disintegration**
- QGSjet 4 II: Overall rather **bad fit**

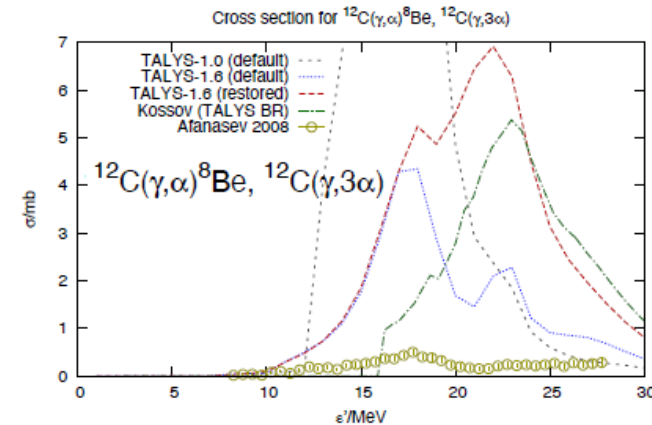
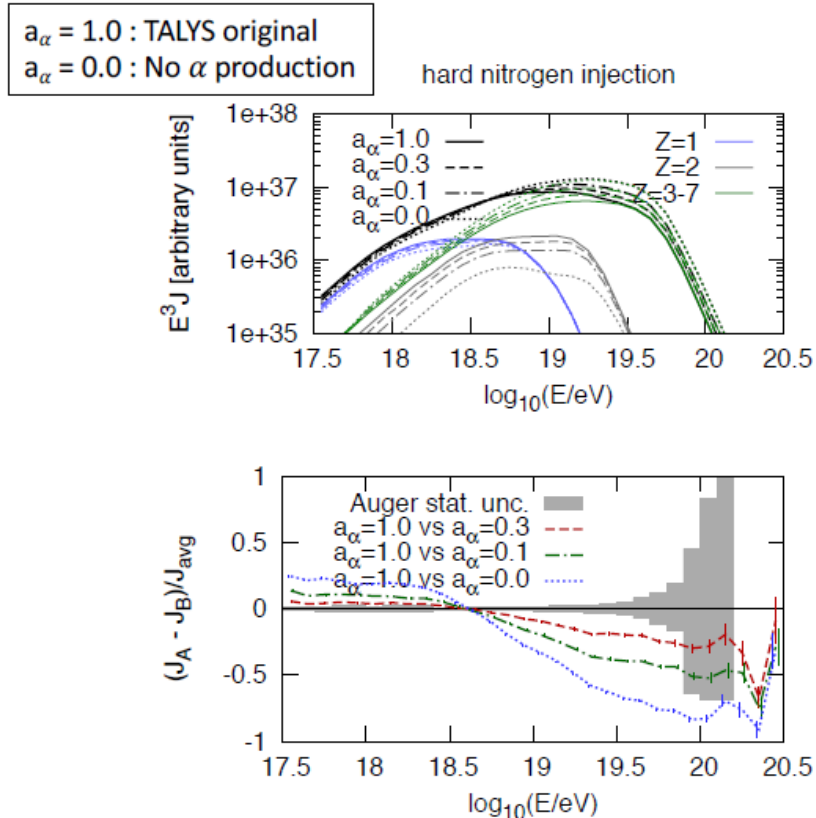
See also: Auger Collaboration JCAP02(2013)026
Auger Collaboration JCAP04(2017)038

The shower model has a stronger qualitative impact!



Forward-folding analysis : Propagation, model dependence

R.A. Vatista et al., JCAP10(2015)063



- **>50% effect of α production rate**, which is poorly constrained by the laboratory experiments, or poorly modeled for existing data (plot above)

$$dN/dE \propto E_{inj}^{-\gamma} \exp(-E_{inj}/ZR_{cut})$$

$$0 < z < 1$$

$$\gamma = 1, R_{cut} = 5 \times 10^{18} \text{ V}$$

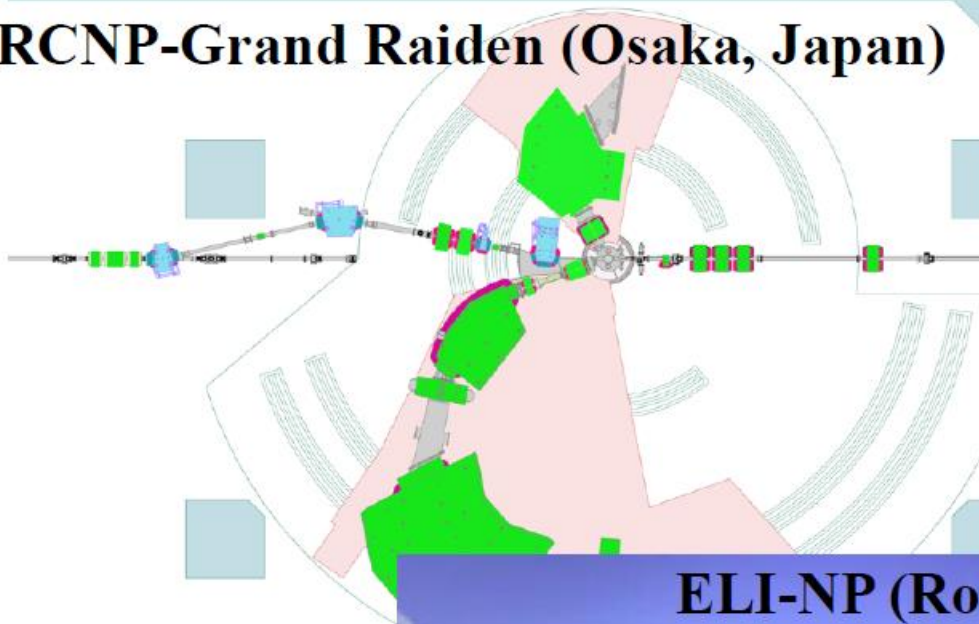
PANDORA Project

Photo-Absorption of Nuclei and Decay Observation for Reactions in Astrophysics

XSCRC2019 Tamii

Joint project among three experimental facilities with nuclear theories and astrophysical simulations

RCNP-Grand Raiden (Osaka, Japan)

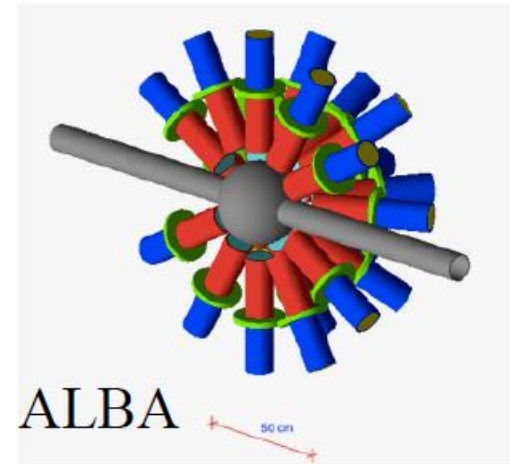


ELI-NP (Romania)



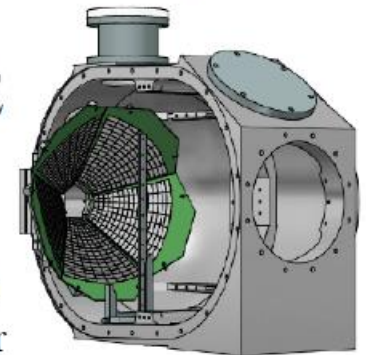
complementary
experimental
techniques

iThemba LABS South Africa



CAKE

decay
charge
particle
detector
array



Schedule of the Measurements

Virtual Photon Exp.

RCNP 2022-

JPS2020 Tamii

Total strength distribution up 32 MeV

γ -decay

multipole decomp. analysis (ang. dep. and polarization transfer)

iThemba LABS 2021-

Beam time approved for the first cases: ^{12}C , ^{27}Al

Total strength distribution up 24 MeV

σ_{abs} and p, α, γ decays

p, α, γ -decays

multipole decomp. analysis (ang. dep.)

Real Photon Exp.

LoI submitted

ELI-NP 2023-

absolute c.s.

model independent separation of E1 and M1

n, p, α, γ -decays up to 20 MeV

Good systematic data

Consistency among three facilities

Reference target: ^{27}Al .

Target Nuclei

Measurements on 10-20 nuclei in 5-10 years
with theoretical model developments

JPS2020 Tamii

Cross section accuracy:
5-10%

Candidate target nuclides

- ^{12}C , ^{16}O , and ^{27}Al first cases, alpha decay, reference target
- ^6Li , ^7Li , ^9Be light nuclei
- (^{20}Ne) , ^{24}Mg , ^{28}Si , ^{32}S , (^{36}Ar) , ^{40}Ca N=Z nuclei, α -cluster effect, deformation
- ^{26}Mg , ^{48}Ca , ^{56}Fe N>Z nuclei
- ^{13}C , ^{14}N , ^{51}V odd and odd-odd nuclei
- (γ, xn) on ^{18}O , ^{48}Ca , ^{64}Ni

Sensitivity test and selection of important nuclei are under discussions.

PANDORA Project: Organization

Nuclear Experiments

JPS2020 Tamii

RCNP

Osaka Univ.

A. Tamii, N. Kobayashi, T. Sudo, Z. Yang, T. Furuno, M. Murata, A. Inoue, H. Mori
ELI-NP

ELI-NP

P.-A. Söderström, D. Balabanski, L. Capponi, A. Dhal, T. Petruse, D. Nichita, Y. Xu
iThemba LABS, Univ. Witwatersrand, Stellenbosh Univ.

iThemba LABS

L. Pellegrini, R. Neveling, F.D. Smit, J.A.C. Bekker, S. Binda, H. Jivan, T. Khumal, M. Wiedeking, K.C.W. Ki, P. Adsley, L.M. Donaldson, E. Sideras-Haddado, K.L. Malatji, S. Jongile, A. Netshiya

TU-Darmstadt

P. von Neumann-Cosel, N. Pietralla, J. Isaak, J. Kleemann, M. Spall

U. Milano/INFN

A. Bracco, F. Camera, F. Crespi, O. Wieland

Nuclear Theory

AMD

M. Kimura, Y. Taniguchi, H. Motoki [Antisymmetrized Molecular Dynamics](#)

NRFT

E. Litvinova, P. Ring, H. Wibowo [Nuclear Relativistic Field Theory](#)

RPA/DFT

T. Inakura

TALYS

S. Goriely, E. Khan

UHECR Theory

Propagation
and production

D. Allard, B. Baret, I. Deloncle, J. Kiener, E. Parizot, V. Tatischeff

S. Nagataki, E. Kido, J. Oliver, H. Haoning

NC Neutrino Detection Y. Koshio, M. Sakuda, M.S. Reen,

PANDORA Project: Organization

Nuclear Experiments

JPS2020 Tamii

RCNP

Osaka Univ.

A. Tamii, N. Kobayashi, T. Sudo, Z. Yang, T. Furuno, M. Murata, A. Inoue, H. Mori
ELI-NP

ELI-NP

P.-A. Söderström, D. Balabanski, L. Capponi, A. Dhal, T. Petruse, D. Nichita, Y. Xu
iThemba LABS, Univ. Witwatersrand, Stellenbosh Univ.

iThemba LABS

L. Pellegrini, R. Neveling, F.D. Smit, J.A.C. Bekker, S. Binda, H. Jivan, T. Khumal, M. Wiedeking, K.C.W. Ki, P. Adsley, L.M. Donaldson, E. Sideras-Haddado, K.L. Malatji, S. Jongile, A. Netshiya

TU-Darmstadt

P. von Neumann-Cosel, N. Pietralla, J. Isaak, J. Kleemann, M. Spall

U. Milano/INFN

A. Bracco, F. Camera, F. Crespi, O. Wieland

Nuclear Theory

AMD

M. Kimura, Y. Taniguchi, H. Motoki **Antisymmetrized Molecular Dynamics**

NRFT

E. Litvinova, P. Ring, H. Wibowo **Nuclear Relativistic Field Theory**

RPA/DFT

T. Inakura

TALYS

S. Goriely, E. Khan

Theoretical models are needed to include the experimental data **in the simulations of the propagation of UHECRs** → Kido started to compare models with collaborators

UHECR Theory

Propagation
and production

D. Allard, B. Baret, I. Deloncle, J. Kiener, E. Parizot, V. Tatischeff

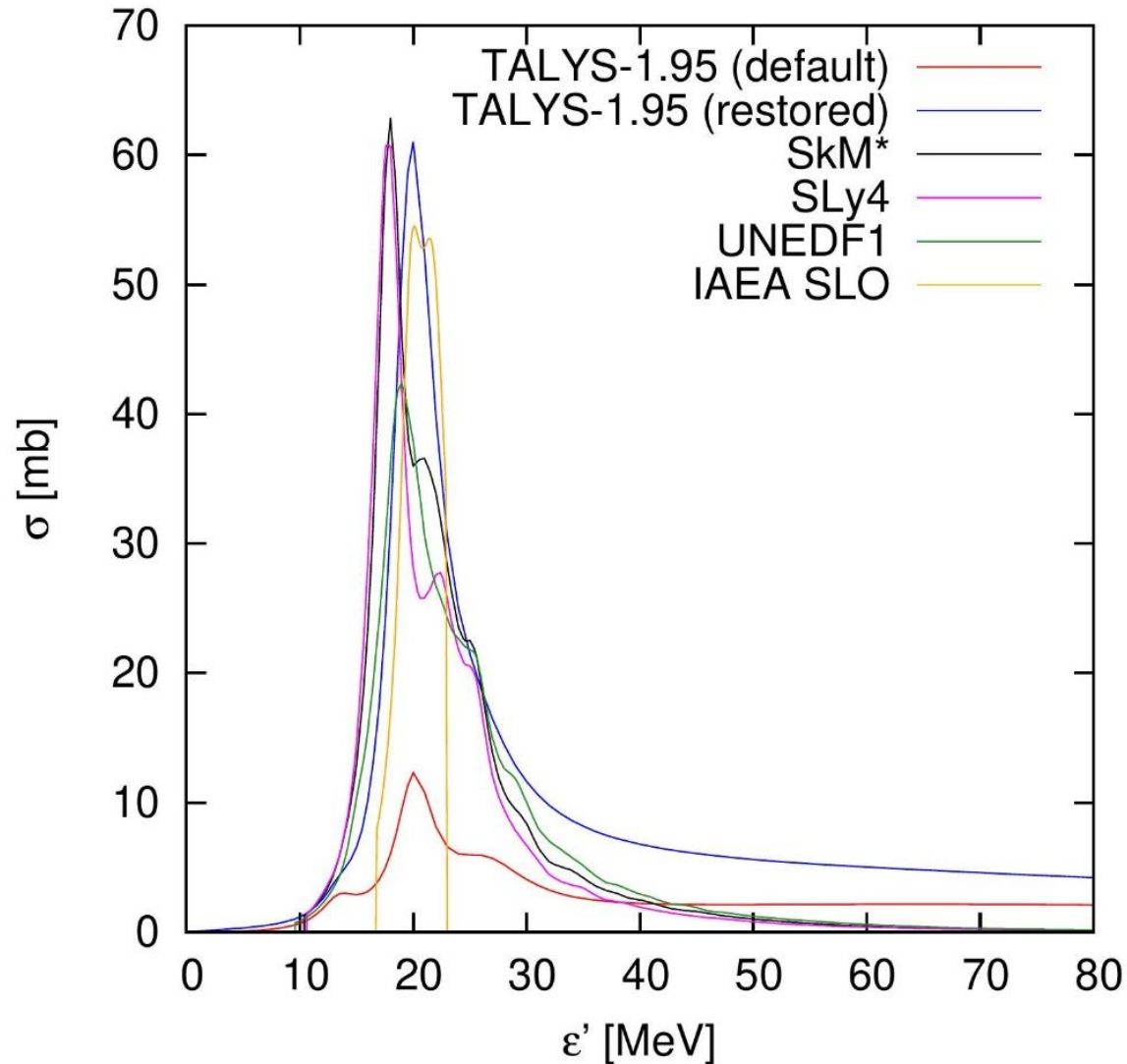
S. Nagataki, E. Kido, J. Oliver, H. Haoning

NC Neutrino Detection Y. Koshio, M. Sakuda, M.S. Reen,

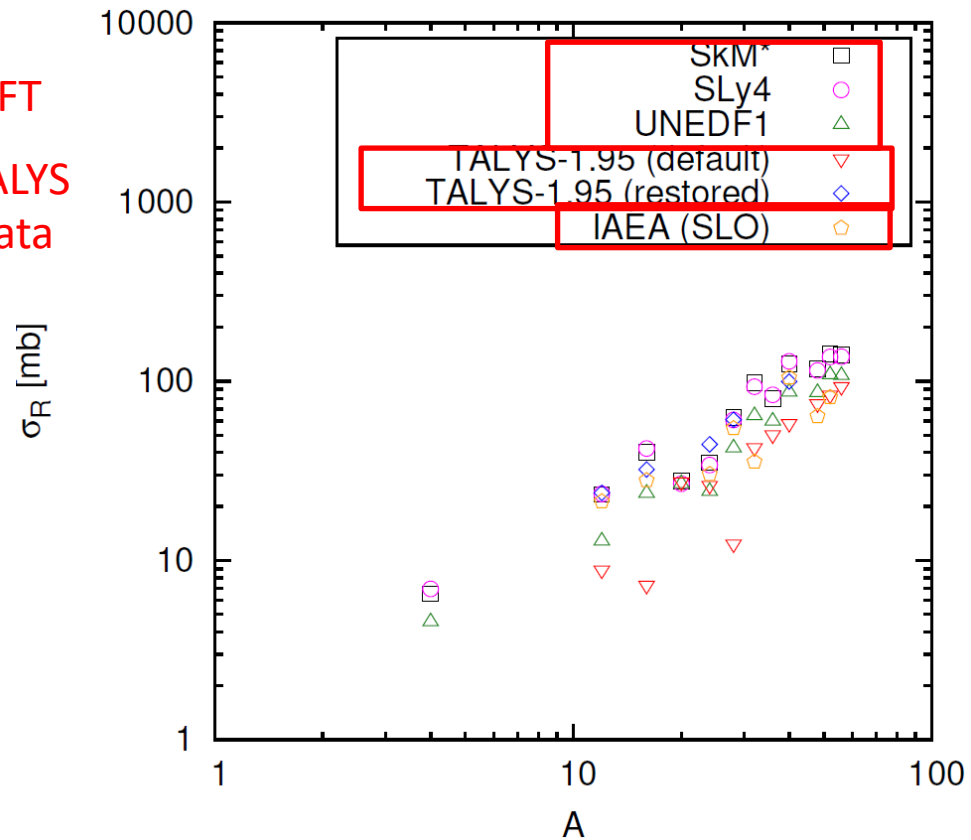
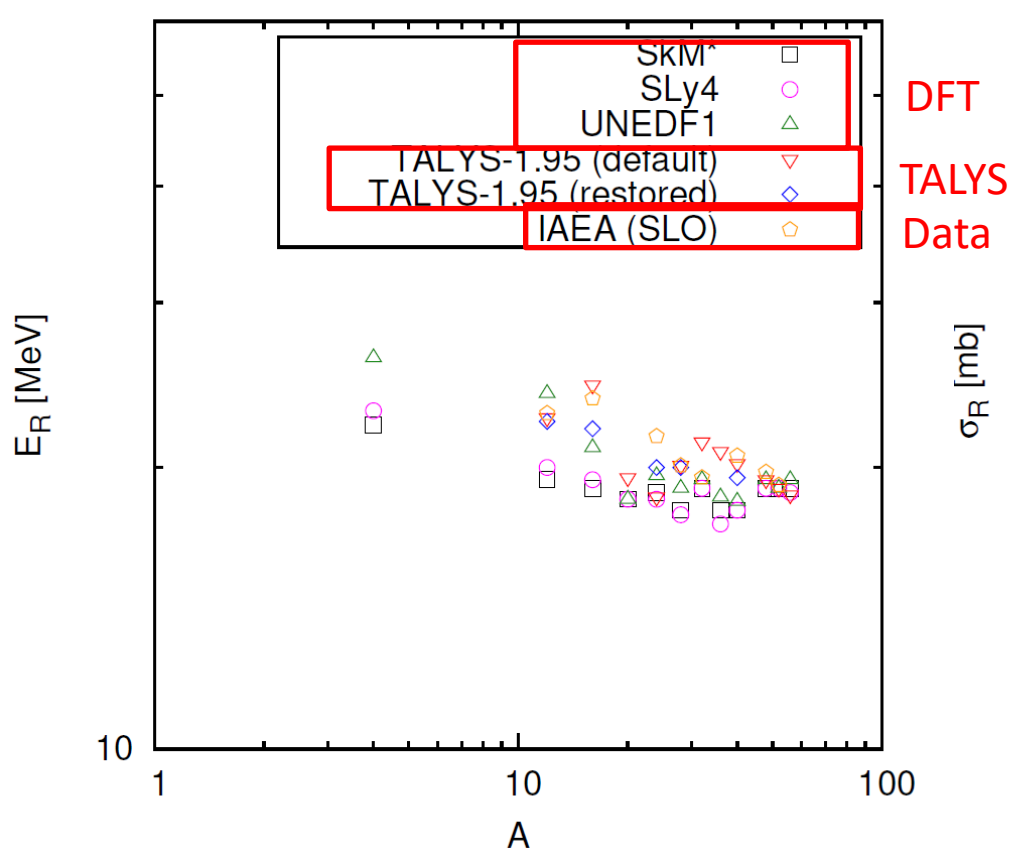
Comparison of Photoabsorption Cross Sections

- T. Inakura *et al.*, *PHYSICAL REVIEW C* **80**, 044301 (2009)
and T. Inakura *et al.*, *PHYSICAL REVIEW C* **84**, 021302(R) (2011).
 - Density Functional Theory (DFT) calculation
 - σ_{GDR} (GDR: Giant Dipole Resonance)
 - 12 nuclei (4He 12C 16O 20Ne 24Mg 28Si 32S 36Ar 40Ca 48Ti 52Cr 56Fe)
 - 3 interaction models
 - SkM* : J. Bartel *et al.*, *Nucl. Phys. A* **386**, 79 (1982).
 - SLy4 : E. Chanbanat, P. Bonche, P. Haensel, J. Mayer, and R. Schaeffer, *Nucl. Phys. A* **627**, 710 (1997).
 - UNEDF1 : M. Kortelainen *et al.*, *Phys. Rev. C* **85**, 024304 (2012).
- TALYS-1.95 https://tendl.web.psi.ch/tendl_2019/talys.html
 - Statistical Hauser-Feshbach theory
 - $\sigma_{\text{GDR}} + \sigma_{\text{QD}}$ (QD: Quasi Deuteron)
 - Default : 11 nuclei
(12C 16O 20Ne 24Mg 28Si 32S 36Ar 40Ca 48Ti 52Cr 56Fe)
 - Restored (E1-strength function was changed for CRPropa and SimProp))
: 5 nuclei (12C 16O 24Mg 28Si 40Ca)
- Data
 - IAEA Photonuclear Data Library 2019 T. Kawano *et al.*
 - Table III Recommended Experimental GDR parameters in the certain energy range
 - Standard Lorentzian (SLO):
$$\sigma_{\text{GDR}}(E_\gamma) = \sigma_R \frac{E_\gamma^2 \Gamma_R^2}{(E_R^2 - E_\gamma^2)^2 + E_\gamma^2 \Gamma_R^2}$$

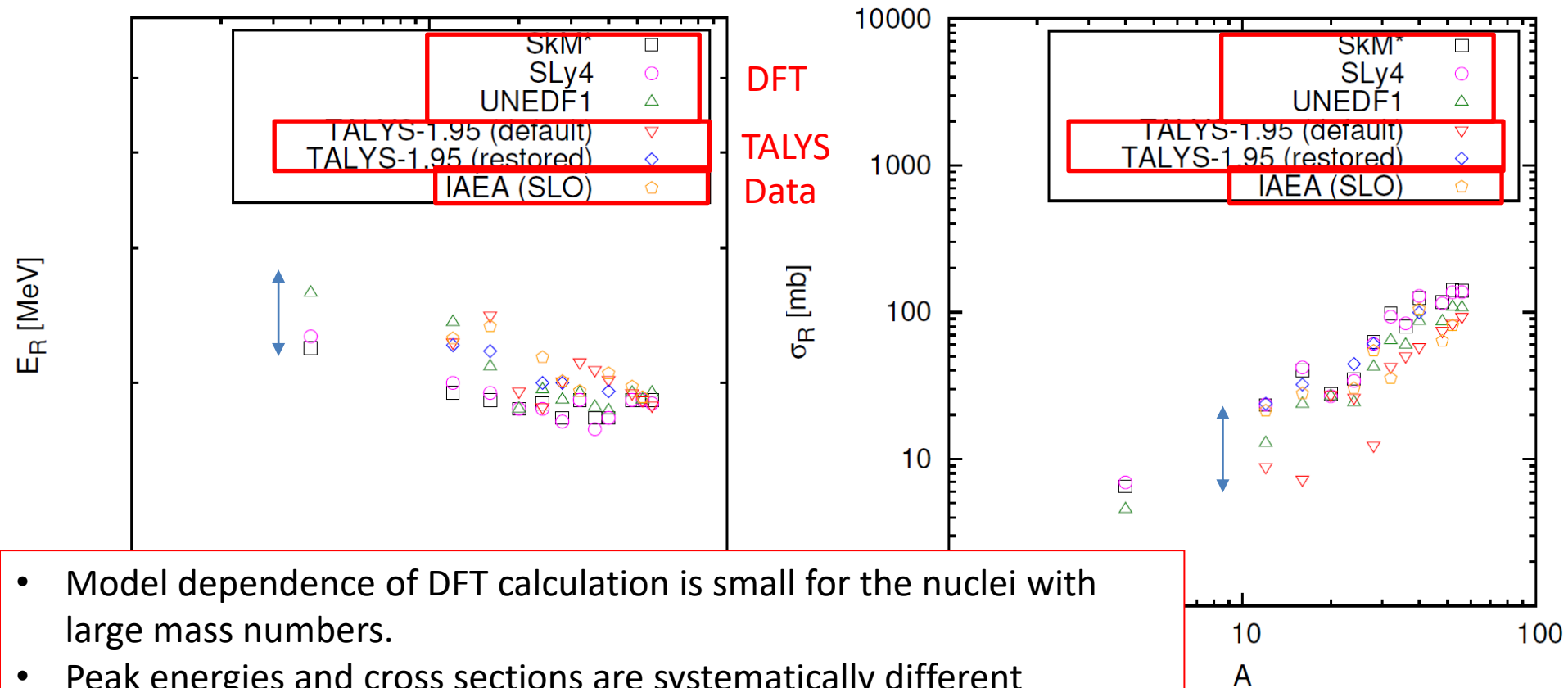
^{28}Si Photoabsorption Cross Sections



Comparison of Peak Energies and Cross Sections

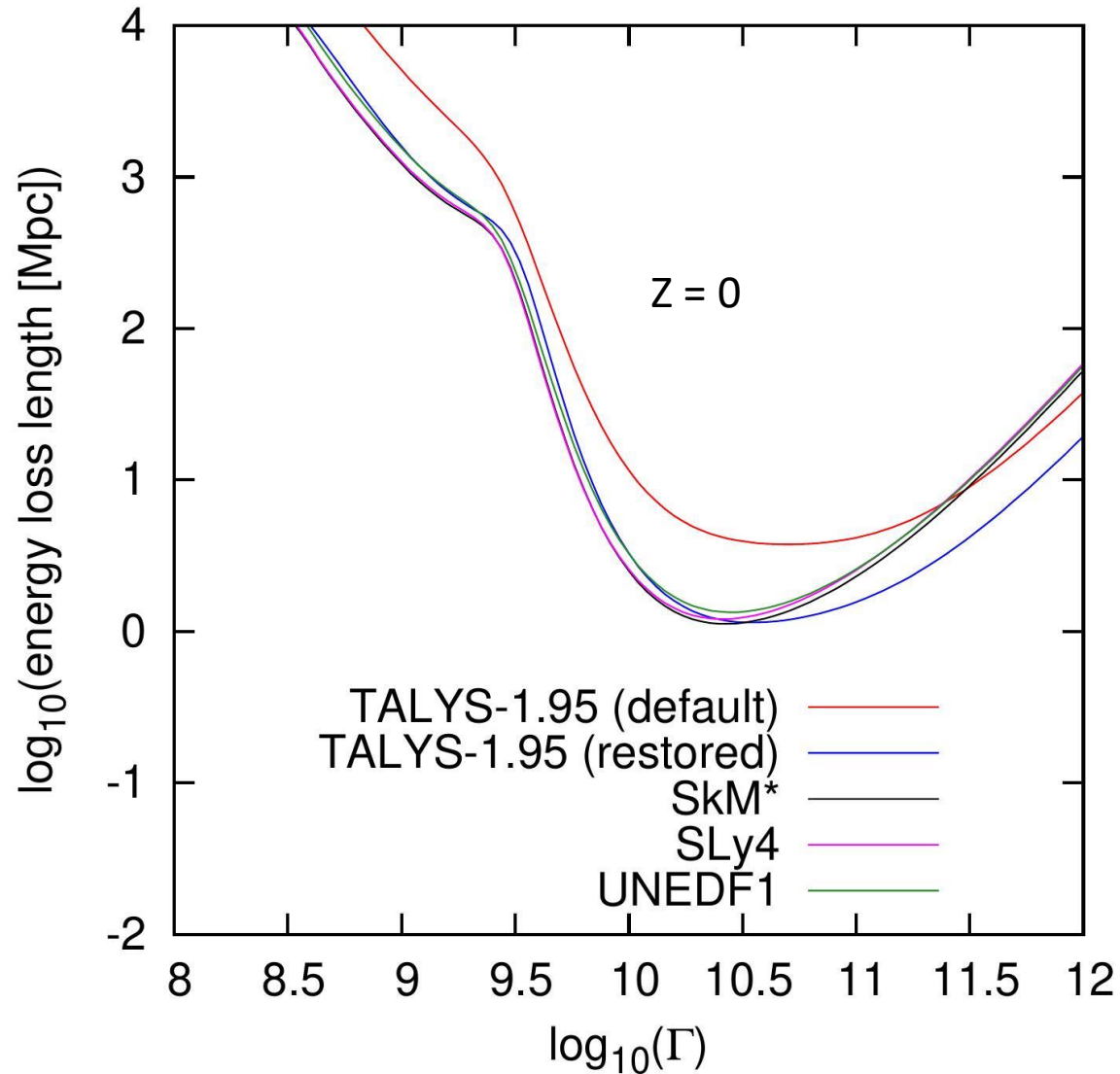


Comparison of Peak Energies and Cross Sections



- Model dependence of DFT calculation is small for the nuclei with large mass numbers.
- Peak energies and cross sections are systematically different depending on the models.

^{28}Si Energy Loss Length of Photodisintegration (CMB + IRB(Gilmore+, 2012))



Simulations of Propagation of UHECRs

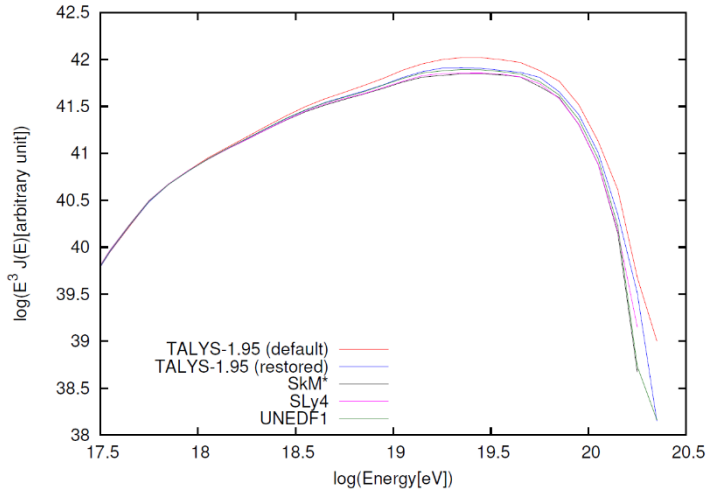
$$dN/dE \propto E_{\text{inj}}^{-\gamma} \exp(-E_{\text{inj}}/Z R_{\text{cut}})$$

$$0 < z < 1$$

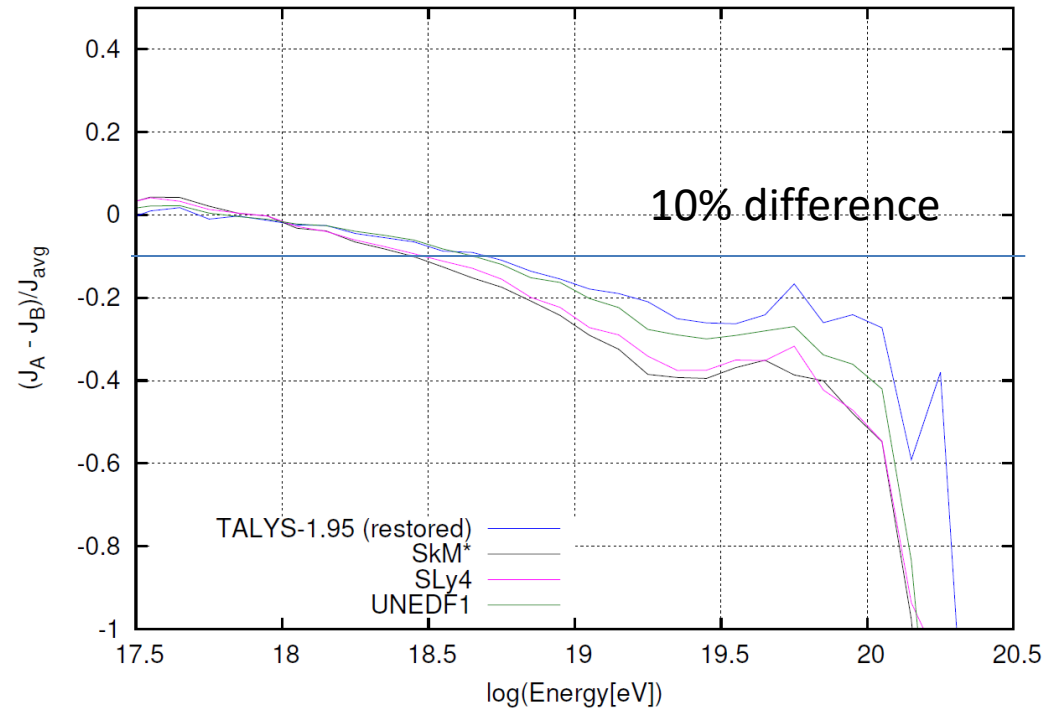
- $\gamma = 1$, $R_{\text{cut}} = 5 \times 10^{18}$ V
- Sources are uniformly distributed in comoving volume.
- CRPropa3
- IRB: Gilmore+ 2012
- 1 dimensional propagation
- We replaced the default mean free path tables (TALYS (restored)) with other models (TALYS (default), SkM*, SLy4, UNEDF1).
- We did not change the tables of the branching ratios.

Energy Spectrum from 28Si source

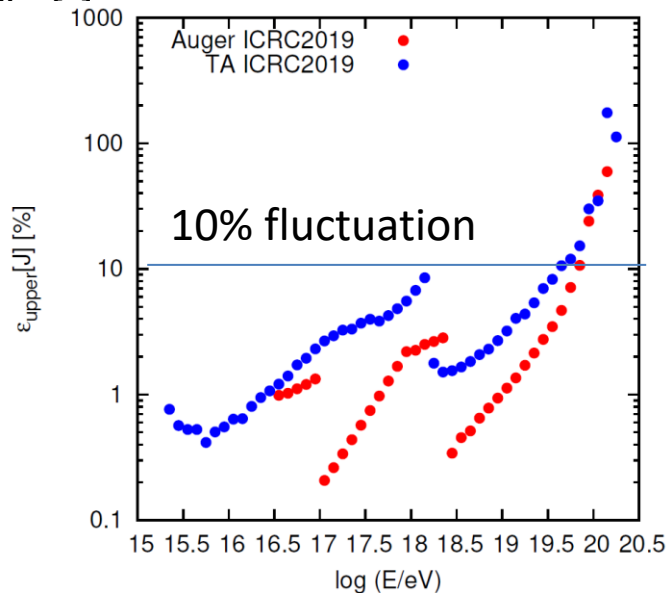
Normalization: total number of events



Comparison of the simulated spectrum with TALYS-1.95 (default) model

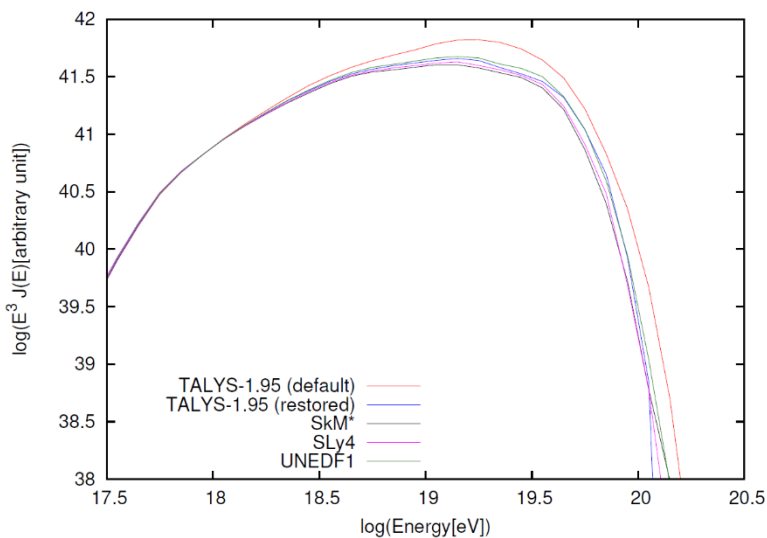


$\sigma[J]/E[J]$ statistical fluctuation of the data

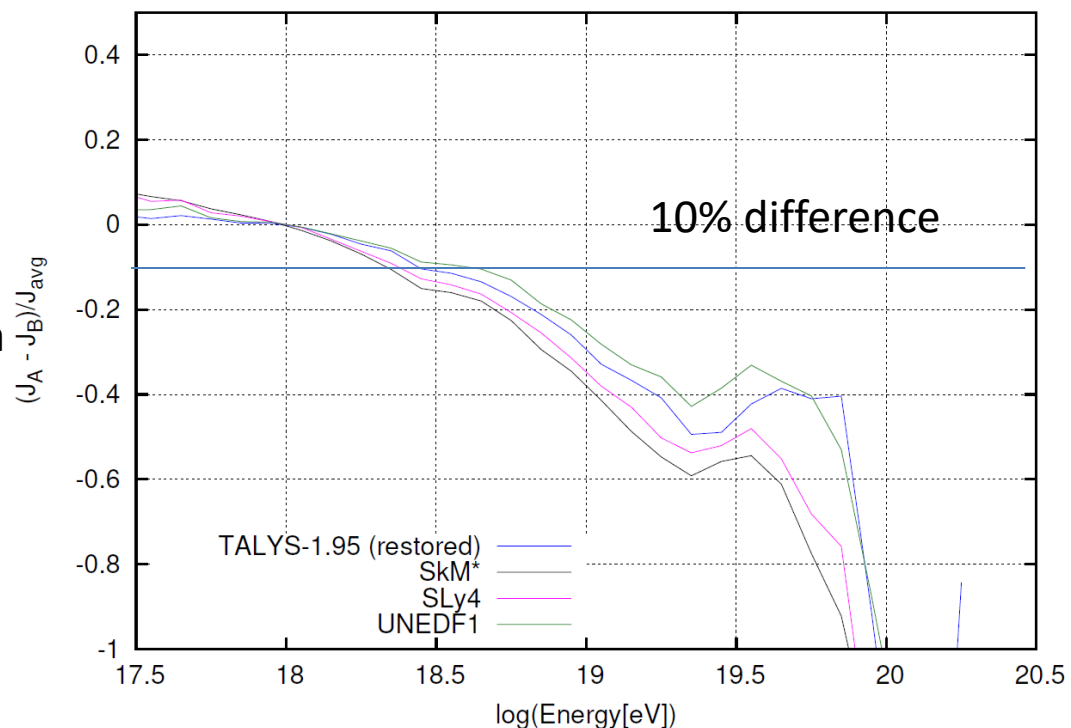


Energy Spectrum from 16O source

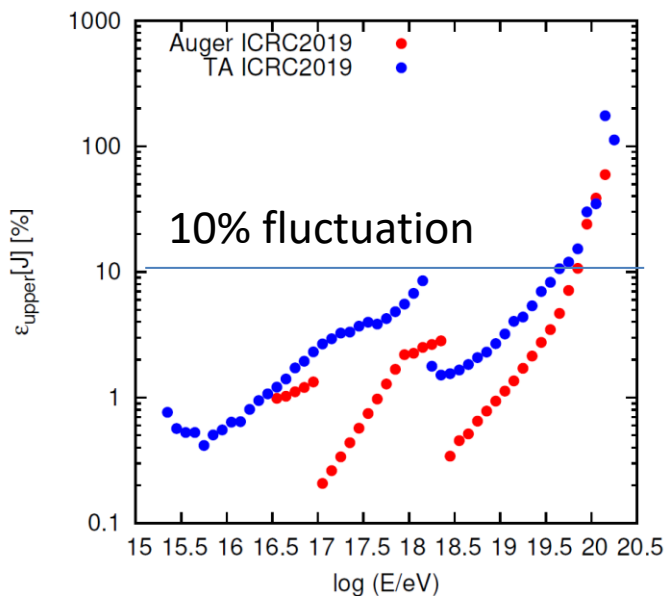
Normalization: total number of events



Comparison of the simulated spectrum with TALYS-1.95 (default) model



$\sigma[J]/E[J]$ statistical fluctuation of the data



Summary

- Uncertainty of X_{\max} is the dominant factor for the interpretation of the experimental data.
- Model dependence of the photo-nuclear interaction models were searched, and especially the uncertainty of the alpha particle production ratio was pointed out by Batista+ 2016.
- PANDORA project will start their measurements in the near future.
- Model dependence of nuclear theories are being studied for the implementation of the measurements in the simulation of propagation of UHECRs.
- Ongoing update from nuclear theorists
 - Cross sections using DFT calculation will be updated by T. Inakura.
 - Cross sections and alpha particle production ratio will be provided using AMD calculation by M. Kimura.

Summary 2

- Intermediate-scale anisotropy
 - TA: **2.9 σ** hotspot, oversampling radius: 25° $E > 57$ EeV
 - Auger: **4.5 σ** correlation with starburst galaxies, oversampling radius: 15° $E > 38$ EeV
- Large-scale anisotropy
 - Auger: dipole was detected in **>5.2 σ** , $E > 8$ EeV in 2017
- Composition
 - TA SD and FD hybrid: consistent with light composition with $\log(E/\text{eV}) > 18.2$ and $\log(E/\text{eV}) < 19.1$
 - Auger: composition becoming lighter up to $2 \cdot 10^{18}$ eV and heavier than this energy
- Energy Spectrum
 - TA: **Declination dependence** was claimed at **4.3 σ** in the energy spectrum
 - Auger: **New flattening feature** was found in the spectral shape at the highest energies
- TAx4 detectors partially started to run.
 - **More than half of TAx4 SDs** were deployed, and **2 TAx4 FD** stations were constructed.
 - **Data acquisition was started.** SD: from **Apr. 2019**, FD: from **Jun. 2018**. Cosmic ray events are being collected.
 - Prospects
 - **$\sim 4 \times$ TA SD** equivalent cosmic ray events with $E > 57$ EeV will be collected when the full operation is started.
 - **$\sim 3 \times$ TA SDFD** equivalent hybrid events will be collected especially for X_{max} at the highest energies when the full operation is started.
- AugerPrime detectors also partially started to run. \rightarrow more composition sensitivity from SDs
- **UHECR source are still uncertain.**
- More information of UHECR sources will be obtained with upgraded experiments!

